

Supported Metallocene Catalysts by Surface Organometallic Chemistry. Synthesis, Characterization, and Reactivity in Ethylene Polymerization of Oxide-Supported Mono- and Biscyclopentadienyl Zirconium Alkyl Complexes: Establishment of Structure/Reactivity Relationships

Michelle Jezequel,[‡] Véronique Dufaud,^{*,‡} Maria José Ruiz-Garcia,[‡] Fernando Carrillo-Hermosilla,[‡] Ute Neugebauer,[‡] Gerald P. Niccolai,[‡] Frédéric Lefebvre,[‡] François Bayard,[‡] Judith Corker,^{§,†} Steven Fiddy,[§] John Evans,[§] Jean-Pierre Broyer,[⊥] Jean Malinge,^{||} and Jean-Marie Basset^{*,‡}

Contribution from the Laboratoire de Chimie Organométallique de Surface, UMR 9986, CNRS-CPE Lyon, 43 Boulevard du 11 Novembre 1918, 69616 Villeurbanne Cédex, France, Department of Chemistry, University of Southampton, Southampton, SO17 1BJ, U.K., Laboratoire de Chimie et Procédés de Polymérisation, 43 Boulevard du 11 Novembre 1918, 69616 Villeurbanne Cédex, France, and ELF-ATOCHEM, Groupement de Recherches de Lacq, B.P. 34 Lacq, 64 170 Artix, France

Received February 25, 2000. Revised Manuscript Received October 23, 2000

Abstract: The reactions of Cp^{*}Zr(CH₃)₃, **1**, and Cp₂Zr(CH₃)₂, **2**, with partially dehydroxylated silica, silica–alumina, and alumina surfaces have been carried out with careful identification of the resulting surface organometallic complexes in order to probe the relationship between catalyst structure and polymerization activity. The characterization of the supported complexes has been achieved in most cases by in situ infrared spectroscopy, surface microanalysis, qualitative and quantitative analysis of evolved gases during surface reactions with labeled surface, solid state ¹H and ¹³C NMR using ¹³C-enriched compounds, and EXAFS. **1** and **2** react with silica(500) and silica–alumina(500) by simple protonolysis of one Zr–Me bond by surface silanols with formation of a single well-defined neutral compound. In the case of silica–alumina, a fraction of the supported complexes exhibits some interactions with electronically unsaturated surface aluminum sites. **1** and **2** also react with the hydroxyl groups of γ-alumina(500), leading to several surface structures. Correlation between EXAFS and ¹³C NMR data suggests, in short, two main surface structures having different environments for the methyl group: [Al]₃–OZrCp^{*}(CH₃)₂ and [Al]₂–OZrCp^{*}(CH₃)(μ-CH₃)–[Al] for the monoCp series and [Al]₂–OZrCp₂(CH₃) and [Al]–OZrCp₂(μ-CH₃)–[Al] for the bisCp series. Ethylene polymerization has been carried out with all the supported complexes under various reaction conditions. Silica-supported catalysts in the absence of any cocatalyst exhibited no activity whatsoever for ethylene polymerization. When the oxide contained Lewis acidic sites, the resulting surface species were active. The activity, although improved by the presence of additional cocatalysts, remained very low by comparison with that of the homogeneous metallocene systems. This trend has been interpreted on the basis of various possible parameters, including the (p-π)–(d-π) back-donation of surface oxygen atoms to the zirconium center.

Introduction

Metallocenes have become increasingly important as Ziegler–Natta catalysts in olefin polymerization since the discoveries reported by Brintzinger and Kaminsky.^{1,2} These systems associate metallocenes and methylaluminoxane (MAO) and exhibit high activities in ethylene, propylene, and higher α-olefins

polymerization.^{1d,3} The novelty of metallocene versus classical (conventional) Ziegler–Natta catalysis is the “single-site” character of the active catalytic species, which leads to the

(2) For recent reviews, see: (a) Kaminsky, W., Ed. *Metalorganic Catalysts for Synthesis and Polymerization: Recent Results by Ziegler–Natta and Metallocene Investigations*; Springer-Verlag: Berlin, 1999. (b) Marks, T. J., Stevens, J. C., Eds. *Topics in Catalysis*; Baltzer: Amsterdam, 1999; Vol. 7, pp 1–208. (c) McKnight, A. L.; Waymouth, R. M. *Chem. Rev.* **1998**, *98*, 2587–2598. (d) Jordan, R. F., Ed. *J. Mol. Catal.* **1998**, *128*, 1–337. (e) Kaminsky, W. *J. Chem. Soc., Dalton Trans.* **1998**, 1413–1418. (f) Janiak, C. In *Metallocene: synthesis, reactivity, applications*; Togni, A., Halterman, R. L., Eds.; Wiley-VCH: New York, 1998; Vol. 2, pp 547–623. (g) Kaminsky, W.; Arndt, M. *Adv. Polym. Sci.* **1997**, *127*, 144–187. (h) Soga, K.; Shiono, T. *Prog. Polym. Sci.* **1997**, *22*, 1503–1546. (i) Bochmann, M. *J. Chem. Soc., Dalton Trans.* **1996**, 255–270. (j) Hamielec, A. E.; Soares, J. B. P. *Prog. Polym. Sci.* **1996**, *21*, 651–706. (k) Fink, G., Mühlhaupt, R., Brintzinger, H. H., Eds. *Ziegler Catalysts*; Springer-Verlag: Berlin, 1995. (l) Brintzinger, H. H.; Fischer, D.; Mühlhaupt, R.; Rieger, B.; Waymouth, R. M. *Angew. Chem., Int. Ed. Engl.* **1995**, *34*, 1143–1170. (m) Möhring, P. C.; Coville, N. J. *J. Organomet. Chem.* **1994**, *479*, 1–29. (n) Jordan, R. F. *Adv. Organomet. Chem.* **1991**, *32*, 325–387.

* To whom correspondence should be addressed.

‡ Laboratoire de Chimie Organométallique de Surface.

§ University of Southampton.

⊥ Laboratoire de Chimie et Procédés de Polymérisation.

|| ELF-ATOCHEM.

† Deceased.

(1) (a) Andresen, A.; Cordes, H. G.; Herwig, H.; Kaminsky, W.; Merk, A.; Mottweiler, R.; Pein, J.; Sinn, H.; Vollmer, H. J. *Angew. Chem., Int. Ed. Engl.* **1976**, *15*, 630–632. (b) Sinn, H.; Kaminsky, W.; Vollmer, H. J.; Woltdt, R. *Angew. Chem., Int. Ed. Engl.* **1980**, *19*, 390–392. (c) Sinn, H.; Kaminsky, W. *Adv. Organomet. Chem.* **1980**, *18*, 99. (d) Kaminsky, W.; Kulper, K.; Brintzinger, H. H.; Wild, F. R. W. P. *Angew. Chem., Int. Ed. Engl.* **1985**, *24*, 507–508.

production of polymers having narrow molecular weight distributions and uniform and tunable microstructures. Much effort has been devoted to the syntheses and characterization of a broad range of new metallocene complexes (note that, more recently, nonmetallocene late transition metal olefin polymerization catalysts⁴ have attracted considerable attention and have exhibited exciting properties). The knowledge derived from these molecular systems allows the tailoring of the polymer properties such as molecular weight and molecular weight distribution as well as stereochemistry through an appropriate ligand design at the metal center.^{1d,2l,3a,5}

The development of these systems was closely linked to the discovery of MAO as a cocatalyst, which is thought to generate a cationic metal alkyl active site by alkylation of the catalyst precursor and abstraction of an anionic ligand.^{2l,n,6} Several molecular cationic zirconocene complexes have been synthesized, some of which exhibit catalytic activity in olefin polymerization in the absence of any cocatalyst.⁷

The character of the anion, that is the conjugate base of the Lewis acid activator, is also thought to be crucial to catalytic activity. A breakthrough in the field of cocatalysts was the discovery of extremely bulky and noncoordinating fluoroarylborane activators,^{7d,e,8–11} leading to highly active cationic catalysts.¹¹

(3) (a) Coates, G. W.; Waymouth, R. M. *Science* **1995**, *267*, 217–219. (b) Gauthier, W. J.; Collins, S. *Macromolecules* **1995**, *28*, 3779–3786. (c) Gauthier, W. J.; Cornigan, J. F.; Taylor, N. J.; Collins, S. *Macromolecules* **1995**, *28*, 3771–3778. (d) Spaleck, W.; Küber, F.; Winter, A.; Rohrmann, J.; Bachmann, B.; Antberg, M.; Dolle, V.; Paulus, E. P. *Organometallics* **1994**, *13*, 954–963. (e) Stehling, U.; Diebold, J.; Kirsten, R.; Röhl, W.; Brintzinger, H. H. *Organometallics* **1994**, *13*, 964–970. (f) Chien, J. C. W.; Llinas, G. L.; Rausch, M. D.; Lin, G.-Y.; Winter, H. H. *J. Am. Chem. Soc.* **1991**, *113*, 8569–8570. (g) Mallin, D. T.; Rausch, M. D.; Lin, G.-Y.; Dong, S.; Chien, J. C. W. *J. Am. Chem. Soc.* **1990**, *112*, 2030–2031. (h) Ewen, J. A.; Jones, R. L.; Razavi, A.; Ferrara, J. D. *J. Am. Chem. Soc.* **1988**, *110*, 6255–6256. (i) Ewen, J. A. *J. Am. Chem. Soc.* **1984**, *106*, 6355–6364.

(4) (a) Gibbs, L. V.; Etherton, B. P.; Hlatky, G. G.; Wang, S. *Proc. Ann. Technol. Conf.—Soc. Plast. Eng.* **1998**, *56* (2), 1871. (b) Britovsek, G. J. P.; Gibson, V. C.; Wass, D. F. *Angew. Chem., Int. Ed.* **1999**, *38*, 428–448. (c) Johnson, L. K.; Killian, C. M.; Brookhart, M. J. *J. Am. Chem. Soc.* **1995**, *120*, 6414. (d) Johnson, L. K.; Killian, C. M.; Arthur, S. D.; Feldman, J.; McCord, E. F.; McLaine, S. J.; Kreutzer, K. A.; Bennett, M. A.; Coughlin, E. B.; Ittel, S. D.; Parthasarathy, A.; Tempel, D. J.; Brookhart, M. S. *PCT Int. Appl.* 96/23010, 1996; *Chem. Abstr.* **1996**, *125*, 222773. (e) Wang, C.; Friedrich, S.; Younkin, T. R.; Li, R. T.; Grubbs, R. H.; Bansleben, D. A.; Day, M. W. *Organometallics* **1998**, *17*, 3149–3151.

(5) (a) Ewen, J. A.; Elder, M. J.; Jones, R. L.; Haspelslagh, L.; Atwood, J. L.; Bott, S. G.; Robinson, K. *Makromol. Chem., Macromol. Symp.* **1991**, *48/49*, 253–295. (b) Welborn, H. C., Jr.; Ewen, J. A. U.S. Patent 5,324,800, 1994; *Chem. Abstr.* **1985**, *102*, 114142. (c) Ewen, J. A. *Stud. Surf. Sci. Catal.* **1986**, *25*, 271.

(6) (a) Sishta, C.; Hathorn, R. M.; Marks, T. J. *J. Am. Chem. Soc.* **1992**, *114*, 1112–1114. (b) Janiak, C.; Riegler, B.; Voelkel, R.; Braun, H.-G. *J. Polym. Sci., Polym. Chem.* **1993**, *31*, 2959–2968.

(7) (a) Bochmann, M.; Jaggar, A. J. *J. Organomet. Chem.* **1992**, *424*, C5–C7. (b) Horton, A. D. *J. Chem. Soc., Chem. Commun.* **1992**, 185–187. (c) Jia, L.; Yang, W.; Stern, C. L.; Marks, T. J. *Organometallics* **1997**, *16*, 842–857. (d) Yang, X.; Stern, C. L.; Marks, T. J. *J. Am. Chem. Soc.* **1994**, *116*, 10015–10031. (e) Yang, X.; Stern, C. L.; Marks, T. J. *J. Am. Chem. Soc.* **1991**, *113*, 3623–3625. (f) Bochmann, M.; Lancaster, S. J.; Hursthouse, M. B.; Abdul Malik, K. M. *Organometallics* **1994**, *13*, 2235–2243. (g) Bochmann, M.; Jaggar, A. J.; Nicholls, J. *Angew. Chem., Int. Ed. Engl.* **1990**, *29*, 780–782. (h) Eshuis, J. J. W.; Tan, Y. Y.; Teuben, J. H. *J. Mol. Catal.* **1990**, *62*, 277–287. (i) Taube, R.; Krukowka, L. J. *Organomet. Chem.* **1988**, *347*, C9–C11. (j) Hlatky, G. G.; Turner, H. W.; Eckman, R. R. *J. Am. Chem. Soc.* **1989**, *111*, 2728–2729. (k) Hlatky, G. G.; Eckman, R. R.; Turner, H. W. *Organometallics* **1992**, *11*, 1413–1416.

(8) Ewen, J. A.; Elder, M. J. U.S. Patent 5,561,092, 1996; *Chem. Abstr.* **1996**, *125*, 301814.

(9) (a) Ewen, J. A.; Elder, M. J. U.S. Patent 5,387,568, 1995; *Chem. Abstr.* **1991**, *115*, 136988. (b) Chien, J. C. W.; Tsai, W.-M.; Rausch, M. D. *J. Am. Chem. Soc.* **1991**, *113*, 8570–8571.

(10) (a) Turner, H. W.; Hlatky, G. G.; Eckman, R. R. U.S. Patent 5,198,401, 1993; *Chem. Abstr.* **1995**, *122*, 33815. (b) Yang, X.; Stern, C. L.; Marks, T. J. *Organometallics* **1991**, *10*, 840–842.

Polyethylene, polypropylene, and copolymers are currently produced industrially by metallocene catalysis but still on a relatively small scale. Several problems still exist, such as the difficulty in controlling polymer morphology with soluble catalysts and sometimes the large amounts of MAO needed to achieve maximum catalytic activity. A greater impact of metallocene catalysis on production is now facilitated by the heterogenization of the systems, which allows these catalysts to be integrated into current metallocene processes.

Three main methods have been developed to support homogeneous systems and are fully detailed in the literature and in recent review articles.^{12–15}

Although the heterogeneous systems have some advantages over the homogeneous metallocenes, the activity of the supported systems is generally reduced with respect to that of homogeneous systems.¹⁶ Only a few detailed structural studies on the active species formed in such systems have been reported. Determination of active site structure could be crucial in the understanding of the catalysts behavior. In the 1980s, Marks

(11) (a) Chen, E. Y.; Marks, T. J. *Chem. Rev.* **2000**, *100*, 1391–1434. (b) Chan, M. S.; Vanka, K.; Pye, C. C.; Ziegler, T. *Organometallics* **1999**, *18*, 4624–4636. (c) Duchateau, R.; Abbenhuis, H. C. L.; van Santen, R. A.; Meetsma, A.; Thiele, S. K.-H.; van Tol, M. F. H. *Organometallics* **1998**, *17*, 7, 5663–5673. (d) Duchateau, R.; van Santen, R. A.; Yap, G. P. A. *Organometallics* **2000**, *19*, 809–816. (e) Marks, T. J. *Acc. Chem. Res.* **1992**, *25*, 57–62. (f) Deck, P. A.; Beswick, C. L.; Marks, T. J. *J. Am. Chem. Soc.* **1998**, *120*, 1772–1784. (g) Ewen, J. A.; Elder, M. J. *Makromol. Chem., Macromol. Symp.* **1993**, *66*, 179–190. (h) Chien, J. C. W.; Song, W.; Rausch, M. J. *Polym. Sci., Part A: Polym. Chem.* **1994**, *32*, 2387–2393.

(12) (a) Hlatky, G. G. *Chem. Rev.* **2000**, *100*, 1347–1376. (b) Abbenhuis, H. C. L. *Angew. Chem., Int. Ed.* **1999**, *38*, 1058–1060. (c) Chien, J. C. W. *Top. Catal.* **1999**, *7*, 23. (d) Kristen, M. O. *Ind. Eng. Chem.* **1999**, *7*, 89. (e) Ribeiro, M. R.; Deffieux, A.; Portela, M. F. *Ind. Eng. Chem. Res.* **1997**, *36*, 1224–1237. (f) Arai, T.; The Ban, H.; Uozumi, T.; Soga, K. *J. Polym. Sci., Part A: Polym. Chem.* **1998**, *36*, 421–428.

(13) (a) Soga, K.; Park, J. R.; Shiono, T. *Polym. Commun.* **1991**, *32*, 310–313. (b) Kaminaka, M.; Soga, K. *Makromol. Chem., Rapid Commun.* **1991**, *12*, 367–372. (c) Kaminaka, M.; Soga, K. *Polym. Commun.* **1992**, *33*, 1105–1107. (d) Soga, K.; Uozumi, T.; Saito, M.; Shiono, T. *Macromol. Chem. Phys.* **1994**, *195*, 1503–1515. (e) Kaminaka, M.; Soga, K. *Macromol. Chem. Phys.* **1994**, *195*, 1369–1373. (f) Sacchi, M. C.; Tritto, D. Z.; Locatelli, P. *Macromol. Rapid Commun.* **1995**, *16*, 581–590. (g) Kaminsky, W. *Macromol. Symp.* **1995**, *89*, 203–219. (h) Lee, D.-H.; Yoon, K.-B.; Noh, S.-K. *Macromol. Rapid Commun.* **1997**, *18*, 427–431. (i) Lee, D.-H.; Lee, H.-B.; Noh, S. K.; Song, B. K.; Hong, S. M. *J. Appl. Polym. Sci.* **1999**, *71*, 1071–1080. (j) Dufrenne, N. G.; Blitz, J. P.; Mevarden, C. C. *Microchem. J.* **1997**, *55*, 192. (k) dos Santos, J. H. Z.; Krug, C.; da Rosa, M. B.; Stedile, F. C.; Dupont, J.; Forte, M. de C. *J. Mol. Catal. A* **1999**, *139*, 199.

(14) (a) Soga, K. *Catal. Des. Tailor-Made Polyolefins, Proc. Int. Symp. (Stud. Surf. Sci. Catal.)* **1994**, 307–314. (b) Iiskola, E. I.; Timonen, S.; Pakkanen, T. T.; Härkki, O.; Lehmus, P.; Seppälä, J. V. *Macromolecules* **1997**, *30*, 2853–2859. (c) Iiskola, E.; Timonen, S.; Pakkanen, T. *Eur. Pat. Appl.* 799,838, 1997; *Chem. Abstr.* **1997**, *127*, 293769. (d) Soga, K.; Kim, H.; Shiono, T. *Macromol. Chem. Phys.* **1994**, *195*, 3347. (e) Soga, K. *Macromol. Symp.* **1995**, *89*, 249. (f) Soga, K. *Macromol. Symp.* **1996**, *101*, 281. (g) Spitz, R.; Saudemont, T.; Malinge, J. *Eur. Pat. Appl.* 889,065, 1999; *Chem. Abstr.* **1999**, *130*, 197102. (h) Gila, L.; Proto, A.; Ballato, E.; Vigliarolo, D.; Lugli, G. U.S. Patent 5,846,895, 1998; *Chem. Abstr.* **1998**, *128*, 35163. (i) Soga, K.; Arai, T.; Hoang, B.; Uozumi, T. *Macromol. Rapid Commun.* **1995**, *16*, 905. (j) Soga, K.; Ban, H.; Arai, T.; Uozumi, T. *Macromol. Chem. Phys.* **1997**, *198*, 2779. (k) Stork, M.; Koch, M.; Klapper, M.; Müllen, K.; Gregorius, H.; Rief, U. *Macromol. Rapid Commun.* **1999**, *20*, 210. (l) Alt, H. G. *J. Chem. Soc., Dalton Trans.* **1999**, 1703. (m) Alt, H. G.; Jung, M. *J. Organomet. Chem.* **1999**, *580*, 1. (n) Galan-Fereres, M.; Koch, T.; Hey-Hawkins, E.; Eisen, M. S. *J. Organomet. Chem.* **1999**, *580*, 145.

(15) (a) Chien, J. C. W.; He, D. *J. Polym. Sci., Part A: Polym. Chem.* **1991**, *29*, 1603–1607. (b) Collins, S.; Kelly, W. M.; Holden, D. A. *Macromolecules* **1992**, *25*, 1780–1785. (c) Soga, K.; Kaminaka, M. *Makromol. Chem.* **1993**, *194*, 1745–1755. (d) Kaminsky, W.; Renner, F. *Makromol. Chem., Rapid Commun.* **1993**, *14*, 239–243. (e) Walzer, J. F., Jr. U.S. Patent 5,643,847, 1997 (Exxon Chemical Co.). (f) Ward, D. G.; Carnahan, E. M. *PCT Int. Appl. WO 96/23005*, 1996 (W. R. Grace). (g) Hlatky, G. G.; Upton, D. *J. Macromolecules* **1996**, *29*, 8019–8020. (h) Roscoe, S. B.; Frechet, J. M.; Walzer, J. F.; Diaz, A. *J. Science* **1998**, *280*, 270–272.

(16) Chien, J. C. W. In ref 2b, pp 23–36.

proposed a detailed description of surface organometallic adsorbates for a series of organoactinides, but little work has been done for group IV metallocenes.^{11e,17}

The expanding field of surface organometallic chemistry (SOMC) offers new possibilities in heterogeneous catalysis and particularly in the construction and determination of the structures, at a molecular level, of the supported complexes.¹⁸ The basic philosophy of this area of heterogeneous catalysis is based on the concept that the supported catalyst is a kind of molecular entity. Ideally, one ceases to speak of "the immobilization of a catalyst" or of "the modification of a surface", but rather one considers the entire continuum—support, metal, and ligands—as a quasi-molecular species responding to both the fundamental rules derived from organometallic chemistry and the rules of surface science. Surface organometallic chemistry offers much more precise control of some metal-centered factors such as the oxidation state and coordination geometry of the catalytic site. The stoichiometric nature of SOMC syntheses often leads to catalytic systems with very high percentages of relatively well defined active catalytic sites. The other advantage of SOMC is the ability to create coordinatively unsaturated species that are much more stable than those in solution, which prevents a lot of bimolecular deactivation.

In this publication, we demonstrate that it is possible to design, construct, and fully characterize at the surfaces of oxides well-defined coordination spheres around zirconium which may be suitable for olefin polymerization in the absence of additional cocatalysts (alumoxane or organo-Lewis acid initiator).

A supported metallocene catalyst should have several basic structural characteristics: a strong chemical bond to the support (to avoid leaching), one or two cyclopentadienyl ligands, an alkyl group (the propagation center), and finally, a cationic charge. It may be that the anionic countercharge must be well separated from this ideal structure site in order to achieve maximum catalyst activity.

Alkylmetallocene complexes were chosen as catalyst precursors, and the initial strong chemical bond to the surface can thus be formed by simple protonolysis of an alkyl ligand by a surface hydroxyl group of the supports.

The surface of oxides may also bear some Lewis acid sites,¹⁹ which would allow the formation of cationic metallocenes. By the choice of the right support and dehydroxylation temperature, one may obtain supported alkyl (or halide) complexes for which the vicinity of Lewis acid sites will favor the partial or total transfer of the alkyl (or the halide) from the zirconium to the surface.

Thus, we have chosen supports which have high Lewis acidity: partially dehydroxylated silica—alumina, alumina, and niobia. For comparison, we have also chosen silica, which has no Lewis acidity and which presumably has no ability to extract the alkyl (or the halide) from the coordination sphere of zirconium, at least by Lewis acidity.

(17) (a) He, M.-Y.; Burwell, R. L.; Marks, T. J. *Organometallics* **1983**, *2*, 566–569. (b) He, M.-Y.; Xiong, G.; Toscano, P. J.; Burwell, R. L.; Marks, T. J. *J. Am. Chem. Soc.* **1985**, *107*, 641–652. (c) Toscano, P. J.; Marks, T. J. *J. Am. Chem. Soc.* **1985**, *107*, 653–659. (d) Hedden, D.; Marks, T. J. *J. Am. Chem. Soc.* **1988**, *110*, 1647–1649. (e) Dahmen, K. H.; Hedden, D.; Burwell, R. L.; Marks, T. J. *Langmuir* **1988**, *4*, 1212–1214. (f) Finch, W. C.; Gillepsie, R. D.; Hedden, D.; Marks, T. J. *J. Am. Chem. Soc.* **1990**, *112*, 6221–6232. (g) Ahn, H.; Marks, T. J. *J. Am. Chem. Soc.* **1998**, *120*, 13533–13534.

(18) Lefebvre, F.; Thivolle-Cazat, J.; Dufaud, V.; Niccolai, G. P.; Basset, J.-M. *Appl. Catal. A: General* **1999**, *182*, 1–8.

(19) (a) Kung, H. H. In *Transition Metal Oxides*; Delmon, B., Yates, J. T., Eds.; Studies in Surface Science and Catalysis 45; Elsevier: Amsterdam, 1989; pp 72–90. (b) Tanabe, K.; Misono, M.; Ono, Y.; Hattori, H. In *New Solid Acids and Bases*; Delmon, B., Yates, J. T., Eds.; Studies in Surface Science and Catalysis 51; Elsevier: Amsterdam, 1989; pp 1–211.

One should note that supported metallocene complexes would be less mobile than the analogous molecules in solution. In classical organometallic chemistry, molecular motion prevents ion pair separation; this effect is overcome by the use of noncoordinating anions (e.g., PF_6^- ,²⁰ $\text{B}(\text{C}_6\text{F}_5)_4^-$,^{7a}). A surface may, as a factor of its rigidity, favor the separation of the cation from the anion.

Thus, this report describes the synthesis and characterization of mono- and biscyclopentadienyl complexes of zirconium grafted on silica, silica—alumina, alumina, and in some cases niobia in order to obtain different coordination spheres and environments of mono- and biscyclopentadienyl zirconium complexes σ -bonded to the surface oxygens. The characterization of the supported complexes has been achieved by in situ infrared spectroscopy, surface microanalysis, qualitative and quantitative analysis of evolved gases during surface reactions, solid-state NMR using ^{13}C -enriched compounds, and EXAFS. The catalytic activity in ethylene polymerization of these surface complexes is also reported. Finally, structure—activity relationships are discussed.

Results

I. Synthesis and Characterization of Surface Cyclopentadienyl Zirconium Alkyl Complexes. I.A. Reaction of $\text{Cp}^*\text{Zr}(\text{CH}_3)_3$ with Partially Dehydroxylated Oxides. Silica.

The silica used in our study is a flamed, nonporous silica with a specific surface of 200 m^2/g (Degussa Aerosil 200). The silica surface presents silanol groups and siloxane bridges which are relatively inert, with the exception of siloxanes in very strained four-member rings. During the condensation process, the surface structure varies in terms of both the nature of these sites and their relative proportions. For example, with increasing temperature of dehydroxylation, silanols are more and more isolated while more and more strained siloxane cycles are formed.²¹ At 500 °C, the concentration of hydroxyl groups of the silica was determined to be 1.2 OH/nm^2 by quantitative solid-state ^1H NMR and by reaction with CH_3Li .²²

When $\text{Cp}^*\text{Zr}(\text{CH}_3)_3$ ($\text{Cp}^* = \eta^5\text{-C}_5\text{Me}_5$), referred to herein as **1** (for a detailed explanation of the numbering scheme, refer to note 23), was sublimed onto a disk of silica (30 mg) which had been dehydroxylated at 500 °C ($\text{SiO}_2(500)$), the infrared band attributed to isolated silanol groups at 3747 cm^{-1} disappeared totally at room temperature. At the same time, bands appeared in the regions of 3100–2700 and 1500–1350 cm^{-1} , which are attributed to $\nu(\text{C-H})$, $\nu(\text{C-C})$, and $\delta(\text{C-H})$ vibrations of the Cp^* ligand and Zr—methyl groups. Excess **1** was removed by sublimation under vacuum (10^{-4} Torr) at room temperature.²⁴ No color change of the white disk was observed.

(20) Jordan, R. F.; Dasher, W. E.; Echols, S. F. *J. Am. Chem. Soc.* **1986**, *108*, 8, 1718–1719.

(21) (a) Morrow, B. A. In *Spectroscopic Characterization of Heterogeneous Catalysts*; Fierro, J. L., Ed.; Studies in Surface Science and Catalysis 57; Elsevier: Amsterdam, 1990; Chapter 3, p A161. (b) Boehm, H. P.; Knözinger, H. In *Catalysis Science and Technology*; Anderson, J. R., Boudart, M., Eds.; Springer-Verlag: Berlin, 1983; Vol. 4, p 39.

(22) Lefebvre, F. Unpublished results.

(23) The following system of abbreviations is used throughout the paper: The molecular precursors, $\text{Cp}^*\text{Zr}(\text{CH}_3)_3$ and $\text{Cp}_2\text{Zr}(\text{CH}_3)_2$ are referred to as **1** and **2**, respectively. Surface complexes are abbreviated as in **1-SiO₂-Al₂O₃(500)**, which refers to precursor **1** grafted to silica—alumina which had been dehydroxylated at 500 °C. Note that the abbreviation can refer to a variety of surface structures in cases where there are several types of surface/precursor binding modes possible. Isotopically labeled complexes are indicated as in **1-¹³C-SiO₂-Al₂O₃(500)**.^{13C}.

(24) Indeed, the band at 2838 cm^{-1} (typical of the $\nu(\text{C-H})$ vibrations of the Zr—Me groups of the molecular compound **1**) had totally disappeared, which indicated that no more molecular complex was physisorbed at the surface.

Table 1. Infrared Data and Assignments of the Molecular Complex Cp*Zr(CH₃)₃, **1**,^a and of the Analogous Oxide-Supported Complexes^b

bands (values given in cm ⁻¹)	1	1·SiO₂(500)	1·SiO₂-Al₂O₃(500)	1·Al₂O₃(500)	1·Nb₂O₅(300)
$\nu_{\text{as}}(\text{C-H})\text{Cp}^*$	2972, 2945	2978, 2957	2975, 2953	2973, 2952	2959
$\nu_{\text{s}}(\text{C-H})\text{Cp}^*$, $\nu_{\text{as}}(\text{C-H})\text{Zr-Me}$	2913	2912	2915	2915	2921
$2\delta_{\text{as}}(\text{C-H})\text{Cp}^*$	2864	2867	2866	2867	2866
$\nu_{\text{s}}(\text{C-H})\text{Zr-Me}$	2838				
$2\delta_{\text{as}}(\text{C-H})\text{Zr-Me}$	2743	2753		2739	
$\nu(\text{C-C})\text{Cp}^*$	1492, 1436	1493, 1436	1490, 1438	1496, 1435	1491, 1435
$\delta_{\text{as}}(\text{C-H})\text{MeCp}^*$	1453	1457	1454	1459	1452
$\delta_{\text{as}}(\text{C-H})\text{Zr-Me}$	1389	1393	1389 ^c	1400 ^c	1390 ^c
$\delta_{\text{s}}(\text{C-H})\text{MeCp}^*$	1380	1381	1381	1383	1380
$\delta(\text{C-H})\text{Al-Me}$				1200	
$\delta_{\text{s}}(\text{C-H})\text{Zr-Me}$	1122			1123	1122

^a Infrared spectrum in CCl₄. ^b Infrared spectra recorded under vacuum. ^c Shoulder.

The only gaseous product of the reaction was methane, which was qualitatively analyzed by gas chromatography coupled with mass spectroscopy.

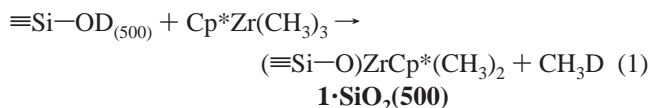
The main infrared bands of the obtained surface species, **1·SiO₂(500)**, and their respective assignments are summarized in Table 1. Most of the vibrations have been interpreted by comparison with the infrared data of molecular compounds such as CpTi(CH₃)₃ and Cp₂Zr(CH₃)₂.²⁵ To discriminate between the zirconium methyl and the cyclopentadienyl methyl vibrations, we repeated the reaction with Cp*Zr(CD₃)₃.²⁶ Bands due to the CD₃ group were observed at 2165, 2071, and 2012 cm⁻¹ (respectively $\nu_{\text{as}}(\text{C-D})$, $\nu_{\text{s}}(\text{C-D})$, and $2\delta_{\text{as}}(\text{C-D})$), and we thus can estimate the position of the Zr-Me vibrations as listed in Table 1 by subtracting the spectrum of the deuterated product from that of the nondeuterated product.

Elemental analysis of the silica disk confirmed the presence of zirconium (3.3–3.5 wt %). This percentage corresponds to 1.1–1.2 Zr/nm², consistent with stoichiometric reaction of all surface silanols with 1 equiv of zirconium.

To perform surface elemental analyses (C, Zr) of the resulting surface species and to facilitate the quantification of the methane evolved during the reaction, we repeated the reaction on a larger scale (500 mg to 1 g). Two different methods were used, depending on the studies considered: (i) sublimation of Cp*Zr(CH₃)₃ at room temperature on the oxide and removal of the unreacted complex at the same temperature under vacuum and (ii) impregnation of the oxide by a solution of Cp*Zr(CH₃)₃ in dry pentane and removal of the unreacted starting material by washing the solid with the same solvent.²⁷

Methane that evolves during the reaction can be formed either by reaction with the surface or by thermal decomposition of the molecular complex Cp*Zr(CH₃)₃. To distinguish between these two possible reactions, we deuterated the silica(500) before the grafting of Cp*ZrMe₃.²⁸ The methane evolved was mono-

deuterated (CH₄-d₁ > 85%), which is a confirmation that the surface reaction occurs between **1** and the surface silanols. The quantity of methane-d₁ evolved per mole of grafted zirconium was found to be 0.9 mol of CH₃D/mol of Zr, again consistent with a 1:1 stoichiometric reaction of the zirconium complex with surface silanols. No liberation of pentamethylcyclopentadiene was observed either in the gas phase or in the pentane extracts.²⁹ The carbon/zirconium molar ratio of the surface species in several experiments was found to vary between 11.5 and 12, suggesting that on average one Cp* ligand and two methyl groups per zirconium atom are left:



Further characterization of the surface species was achieved by solid-state NMR spectroscopy.³⁰

The CP-MAS ¹³C NMR spectrum of **1·SiO₂(500)** (Figure 1c) indicated the presence of three signals at 120, 37, and 9 ppm. The signals at 120 and 9 ppm were unambiguously attributed to, respectively, the carbons of the cyclopentadienyl ring and the carbons of the methyl groups of the Cp* ligand. The broad signal at 37 ppm could be attributed to the carbons of the Zr-CH₃ groups.³¹

Since the intensity of this peak was relatively weak (as expected),³² and given the importance of the methyl groups in our study, we undertook the synthesis of the isotopically enriched starting material, Cp*Zr(¹³CH₃)₃. This was cleanly obtained by reaction of Cp*ZrCl₃ with ¹³CH₃MgI.^{31a,33} The ¹³C-{¹H} NMR spectrum (Figure 1b) of Cp*Zr(¹³CH₃)₃ in C₆D₆

(29) To confirm that no pentamethylcyclopentadiene was physisorbed on the silica surface, the solid was washed after reaction with small amounts of dry pentane. The pentane extracts were then analyzed by gas chromatography, and no Cp*H was detected.

(30) ¹H NMR. The solid-state ¹H NMR spectra of **1·SiO₂(500)** and **1·SiO₂-Al₂O₃(500)** showed two large signals each, respectively at 1.7 and -0.3 ppm and 1.5 and -0.6 ppm. The former resonance was attributed to the protons of the methyl groups of the Cp* ligand. We assigned the latter resonance to the protons of the methyl groups directly bonded to the zirconium atom (see ref 31). In the case of the alumina-supported zirconium species, **1·Al₂O₃(500)**, the solid-state ¹H NMR spectrum exhibited only one signal at 2.0 ppm. This resonance was too large to allow one to distinguish between different types of methyl groups, those previously cited as well as species involving the alumina surface (Al-CH₃ and Zr-(μ-CH₃)-Al fragments).

(31) (a) Wolcanski, P. T.; Bercaw, J. E. *Organometallics* **1982**, *1*, 793. (b) Baxter, S. M.; Ferguson, G. S.; Wolcanski, P. T. *J. Am. Chem. Soc.* **1988**, *110*, 4231. (c) Ferguson, G. S.; Wolcanski, P.; Parkanyi L.; Zonneville, M. C. *Organometallics* **1988**, *7*, 1967.

(32) The carbon of the methyl directly bonded to a metal is very often not detected or seen with a very weak intensity in CP-MAS solid-state ¹³C NMR, probably due to a long T₁ relaxation time (phenomenon often seen for organometallics in close proximity to the surface).

(33) Salinger, R.; Mosher, M. *J. Am. Chem. Soc.* **1964**, *86*, 1782.

(25) (a) McGrady, M.; Downs, A. J.; Hamblin, J. M. *Organometallics* **1995**, *14*, 3783–3790. (b) McQuillan, G. P.; McKean, D. C.; Torto, I. *J. Organomet. Chem.* **1986**, *312*, 183–195. (c) Nakamoto, K. In *Infrared and Raman Spectra of Inorganic and Coordination Compounds, Part B: Applications in Coordination Organometallic and Bioinorganic Chemistry*, 5th ed.; John Wiley: New York, 1997; p 286.

(26) Cp*Zr(CD₃)₃ was prepared by reaction of CD₃MgI with Cp*ZrCl₃ in pentane solution at 25 °C; ¹H NMR, C₆D₆, δ 1.76 ppm (s, CH₃ of Cp* ligand); ¹³C{¹H} NMR, C₆D₆, δ 11 ppm (s, CH₃ of Cp* ligand), 119 ppm (s, C of the Cp* ring).

(27) Both preparation methods lead to the formation of the same surface species. The purity of the obtained solids was verified by solid-state ¹³C NMR spectroscopy starting with supported ¹³C-enriched Cp*Zr(¹³CH₃)₃. The spectra of the surface species synthesized by both preparation methods were similar.

(28) The deuteration of the silica was achieved by heating normal SiO₂(500) under D₂O (>90% D, 22 mmHg) at 500 °C for 3–4 h, followed by evacuation at that temperature for 3 h; this procedure was repeated three times before a final dehydroxylation at 500 °C for 15 h. According to infrared data, the silica was deuterated more than 95%.

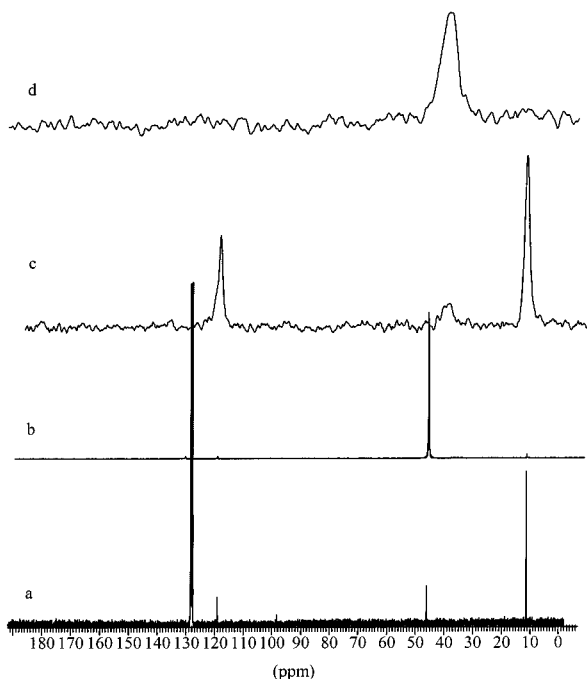


Figure 1. (a) $^{13}\text{C}\{^1\text{H}\}$ NMR spectrum of $\text{Cp}^*\text{Zr}(\text{CH}_3)_3$ in C_6D_6 . (b) $^{13}\text{C}\{^1\text{H}\}$ NMR spectrum of $\text{Cp}^*\text{Zr}(^{13}\text{CH}_3)_3$ in C_6D_6 . (c) CP-MAS ^{13}C NMR spectrum of $\mathbf{1}\cdot\text{SiO}_2(\mathbf{500})$ (Zr, 1.7 wt %). (d) CP-MAS ^{13}C NMR spectrum of $\mathbf{1}\cdot\text{SiO}_2(\mathbf{500})\text{-}^{13}\text{C}$ (Zr, 0.5 wt %).

solution, $\mathbf{1}\text{-}^{13}\text{C}$, exhibits a very intense signal at 48 ppm due to the carbons of the $\text{Zr}\text{-}^{13}\text{CH}_3$ groups. We recognize also at 121 and 14 ppm the signals corresponding to the carbons of respectively the Cp^* ring and the methyl groups of the Cp^* ligand. The complex $\mathbf{1}\text{-}^{13}\text{C}$ was then reacted at room temperature with the silanols of a silica(500). The CP-MAS ^{13}C NMR spectrum of the resulting surface species, $\mathbf{1}\cdot\text{SiO}_2(\mathbf{500})\text{-}^{13}\text{C}$, showed only one peak at 39 ppm, with a high intensity, confirming the attribution of this peak to the carbon of a $\text{Zr}\text{-}^{13}\text{CH}_3$ group (Figure 1d). The significant high-field shift ($\Delta\delta = 9$ ppm) in going from the molecular material to the supported one could indicate that the zirconium atom is more electron rich due to the back-bonding of the surface oxygen atom.^{31b,c,34}

The reaction of $\mathbf{1}$ with the silanols of a silica dehydroxylated at 500 °C leads therefore to the formation of a single supported zirconium species, $(\equiv\text{Si}\text{-O})\text{ZrCp}^*(\text{CH}_3)_2$, $\mathbf{1}\cdot\text{SiO}_2(\mathbf{500})$, in which the zirconium atom is linked to the surface via one zirconium–oxygen σ -bond.

Silica–Alumina. We continued our study by using oxides bearing some Lewis acidity in order to produce more electrophilic supported zirconium complexes. The silica–alumina used here was composed of 75% silica and 25% alumina with a surface area of 374 m^2/g . The infrared spectrum of $\text{SiO}_2\text{-Al}_2\text{O}_3\text{-}(500)$ showed only one sharp band at 3747 cm^{-1} , characteristic of the isolated silanols. In agreement with other studies,³⁵ no $\nu(\text{Al}\text{-OH})$ vibrations have been observed. This can be explained

(34) (a) Jordan, R. F.; Bajgur, C. S.; Dasher, W. E. *Organometallics* **1987**, *6*, 1041. (b) Borkowsky, S. L.; Jordan, R. F.; Hinch, G. D. *Organometallics* **1991**, *10*, 1268. (c) Lubben, T. V.; Wolczanski, P. T. *J. Am. Chem. Soc.* **1987**, *109*, 424. (d) Siedle, A. R.; Newmark, R. A.; Lamanna, W. M.; Schroepfer, J. N. *Polyhedron* **1990**, *9*, 301.

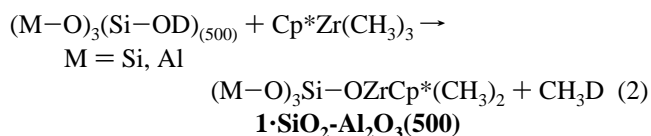
(35) (a) Rouxhet, P. G.; Sempels, R. E. *J. Chem. Soc., Faraday Trans. 1* **1974**, *70*, 2021. (b) Bourne, K. H.; Cannings, F. R.; Pitkethly, R. C. *J. Phys. Chem.* **1970**, *74*, 2197. (c) Peri, J. B. *J. Phys. Chem.* **1966**, *70*, 3368. (d) Basila, M. R. *J. Phys. Chem.* **1962**, *66*, 2223. (e) Iwasawa, Y. In *Tailored Metal Catalysts*; Iwasawa, Y., Ed.; D. Reidel Publishing Co.: Dordrecht, The Netherlands, 1986; p 20. (f) Nédez, C.; Choplin, A.; Lefebvre, F.; Basset, J.-M. *Inorg. Chem.* **1994**, *33*, 1575–1578.

easily. Indeed, during the synthesis and/or the dehydroxylation of silica–alumina, basic $>\text{Al}\text{-OH}$ groups would selectively react with acidic $\equiv\text{Si}\text{-OH}$ groups by condensation to $>\text{Al}\text{-O}\text{-Si}\equiv$ with formation of water.

When $\mathbf{1}$ was sublimed onto the $\text{SiO}_2\text{-Al}_2\text{O}_3(500)$ disk, the silanol band at 3747 cm^{-1} disappeared, with the simultaneous appearance of a group of bands in the spectral regions corresponding to $\nu(\text{C}\text{-H})$, $\nu(\text{C}\text{-C})$, and $\delta(\text{C}\text{-H})$ of the Cp^* ligand and zirconium–methyl groups (3100–2700 and 1500–1350 cm^{-1}) (Table 1). The main reaction on the surface seems to take place between the molecular zirconium complex and the surface silanols. Excess $\mathbf{1}$ was removed under vacuum (10^{-4} Torr) at room temperature. The initially white disk turned light yellow after reaction. The only gaseous product that evolved during the reaction was identified as methane by gas chromatography coupled with mass spectroscopy. No pentamethylcyclopentadiene was detected at the end of the reaction.

All the infrared data of the resulting surface species, $\mathbf{1}\cdot\text{SiO}_2\text{-Al}_2\text{O}_3(\mathbf{500})$, and assignments are summarized in Table 1. The bands are quite similar in shape and frequency to those obtained for $\mathbf{1}\cdot\text{SiO}_2(\mathbf{500})$. However, in the region characteristic of the $\delta(\text{C}\text{-H})$ vibrations (1500–1300 cm^{-1}), a notable difference was seen. In the case of the silica-supported complex, a relatively strong and sharp band, attributed to the $\delta_{\text{as}}(\text{C}\text{-H})$ of the $\text{Zr}\text{-methyl}$ groups, was observed at 1393 cm^{-1} , but in the case of the silica–alumina-supported complex, this vibration was weak and centered at 1389 cm^{-1} .

Surface elemental analysis carried out on the disk after the infrared experiments confirmed the presence of zirconium (3.2 wt %). To determine the stoichiometry of the reaction, the methane liberated was quantified by using a larger amount of silica–alumina (1 g) that had been previously deuterated. The carbon/zirconium molar ratio (11.5–11.8 C/Zr) obtained for the surface species suggests that the silica–alumina-supported organozirconium fragment bears, on average, one Cp^* ligand and two methyl groups (expected 12 if one methyl group is substituted with a siloxy group). Methane- d_1 (1.1 mol/mol Zr) was liberated during the course of the reaction, confirming the elemental analysis. The reaction which took place with the silica–alumina surface occurred principally with the surface silanols and seemed very similar to that observed on silica. It can be formulated as in eq 2.



Further characterization was achieved by solid-state NMR spectroscopy.³⁰

The CP-MAS ^{13}C NMR spectrum (Figure 2b) of the ^{13}C -enriched surface species, $\mathbf{1}\cdot\text{SiO}_2\text{-Al}_2\text{O}_3(\mathbf{500})\text{-}^{13}\text{C}$, exhibited three sharp signals at 120, 37, and 10 ppm and a broad signal at -4 ppm. The signals at 120 and 10 ppm are characteristic respectively of the carbons of the Cp^* ring and of the methyl groups of the Cp^* ligand. The intensities of these signals, as expected for natural abundance, are weak compared to that of the signal at 37 ppm, which corresponds to the carbons of enriched $\text{Zr}\text{-}^{13}\text{CH}_3$ groups. This resonance is shifted to high fields with respect to the $\text{Zr}\text{-}^{13}\text{CH}_3$ resonance of the starting molecular compound (δ 48 ppm). The broad signal at -4 ppm could be attributed to the carbons of some methyl groups in interaction with a Lewis functionality of the surface.³⁶ The broadening is probably due to interaction with (or proximity

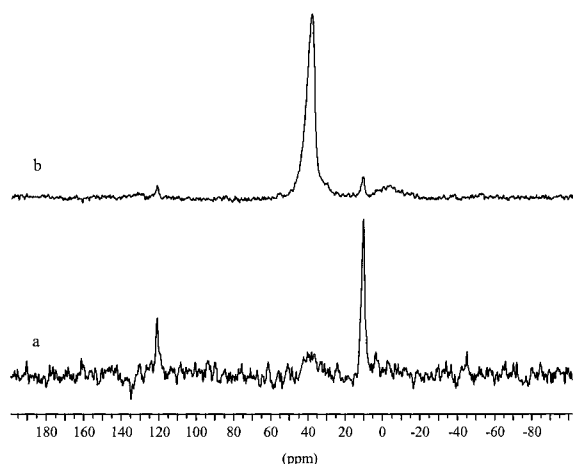
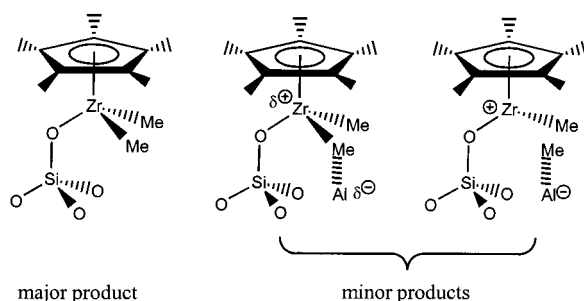


Figure 2. CP-MAS ^{13}C NMR spectra of (a) $1\cdot\text{SiO}_2\text{-Al}_2\text{O}_3(500)$ (Zr, 2 wt %) and (b) $1\cdot\text{SiO}_2\text{-Al}_2\text{O}_3(500)\text{-}^{13}\text{C}$ (Zr, 1.74 wt %).

Scheme 1



to) the quadrupolar nucleus of aluminum atoms. Thus, the methyl groups which bridge between a zirconium and an aluminum atom or which are totally transferred to the aluminum center should not be numerous, given the relatively low concentration of aluminum at the surface, which would explain the weak intensity of the signal at -4 ppm.

In summary, the reaction of **1** with a silica–alumina(500) surface leads to the formation of a supported organozirconium species whose general structure can be formulated as $(\equiv\text{SiO})\text{-Zr}(\text{Cp}^*)(\text{CH}_3)_2\cdot 1\cdot\text{SiO}_2\text{-Al}_2\text{O}_3(500)$, in which the zirconium atom is grafted to the surface via one σ -covalent $\text{Zr-O-Si}\equiv$ bond. For some surface species, there are apparently Lewis acidic centers sufficiently close to interact with a zirconium–methyl group, inducing thus a positive (partial or total) charge on the zirconium atom (Scheme 1).

γ -Alumina. The alumina used in our study is a γ -alumina with a surface area of $100\text{ m}^2/\text{g}$. Alumina is a complicated oxide. Its structure has been the subject of a large number of studies in the literature.^{21a,37} Alumina is an ionic solid with different types of aluminum coordination environments. According to the nature of the exposed faces and the temperature of dehydroxylation of the solid, the surface composition of alumina changes. It can be confidently stated that the alumina surface presents several different types of hydroxyl groups³⁸ as well as Lewis acidic, coordinatively unsaturated, Al^+ sites where the aluminum atom is in a trigonal or a pentahedral geometry, associated with

an adjacent Lewis base AlO^- site. These bridges (Al^+ , AlO^-) are formed during the dehydroxylation processes with separated charges due to steric strain and the ionic character of aluminum. There are also some extremely reactive groups (“defect sites”) of multiple vacancies (Al^+) and multiple AlO^- clusters which have exceedingly high Lewis acidities and basicities, respectively.

Reaction of **1** with γ -alumina(500) was carried out at room temperature and followed by infrared spectroscopy.³⁹ Before reaction, the solid exhibited four well-defined bands at 3792 , 3777 , 3730 , and 3688 cm^{-1} , corresponding to the $\nu(\text{OH})$ vibrations of the different types of OH groups. According to the model presented by Knözinger and Ratnasamy,^{37a} the bands at 3792 and 3777 cm^{-1} were attributed respectively to type Ib and Ia terminal hydroxyl groups, the more intense band at 3730 cm^{-1} to type IIa and IIb bridging OH groups, and the band at 3688 cm^{-1} to type III OH groups. On contact with **1**, all the $\nu(\text{OH})$ vibrations disappeared completely, showing thus the very strong reactivity of these five types of OH groups toward the organozirconium compound. Simultaneously, bands appeared in the regions $3100\text{--}2700$ and $1500\text{--}1350\text{ cm}^{-1}$, characteristic of the $\nu(\text{C-H})$, $\nu(\text{C-C})$, and $\delta(\text{C-H})$ vibrations of the Cp^* ligand and the methyl groups of $1\cdot\text{Al}_2\text{O}_3(500)$. Excess **1** was removed under vacuum at room temperature. The final color of the disk was yellow. Methane was the only gaseous product detected during the course of the reaction. In the case of $\text{Cp}^*\text{-Zr}(\text{CD}_3)_3$, bands due to the CD_3 group were observed at 2193 , 2083 , and 2025 cm^{-1} (respectively $\nu_{\text{as}}(\text{C-D})$, $\nu_{\text{s}}(\text{C-D})$, and $2\delta_{\text{as}}(\text{C-D})$). The positions of the Zr-Me vibrations of the resulting surface species, $1\cdot\text{Al}_2\text{O}_3(500)$, could then be interpreted unambiguously as listed in Table 1.

One should note that the well-defined band at 1393 cm^{-1} observed on silica–alumina(500) and the shoulder at 1389 cm^{-1} seen on silica–alumina(500) attributed to $\delta(\text{C-H})$ vibrations of a zirconium–methyl group are much less intense on alumina. This could indicate that the Zr-methyl groups are modified by the presence of an interaction between the zirconium–methyl group and an adjacent Lewis cation of the surface and/or by the complete transfer of some methyl groups to some very acidic sites of the surface. This hypothesis is confirmed by the presence on alumina(500) of a band at 1200 cm^{-1} assigned to a $\delta(\text{C-H})$ vibration of an aluminum–methyl fragment.⁴⁰

The reaction between **1** and alumina(500) was reproduced on a larger scale (1 g), either by sublimation or by impregnation in dry pentane, using a deuterated support. The quantity of

(36) (a) Siedle, A. R.; Newmark, R. A.; Schropfer, J. N.; Lyon P. A. *Organometallics* **1991**, *10*, 400. (b) Waymouth, R. M.; Santarsiero, B. D.; Coots, R. J.; Bronikowski, M. J.; Grubbs, R. H. *J. Am. Chem. Soc.* **1986**, *108*, 1427. (c) Toscano, P. J.; Marks, T. J. *J. Am. Chem. Soc.* **1985**, *107*, 653–659.

(37) (a) Knözinger, H.; Ratnasamy, P. *Catal. Rev. Sci. Eng.* **1978**, *17*, 31. (b) Lippens, B. C.; de Boer, J. H. *Acta Crystallogr.* **1964**, *17*, 1312. (c) Peri, J. B. *J. Phys. Chem.* **1965**, *69*, 220. (d) Morterra, C.; Magnacca, G. *Catal. Today* **1996**, *27*, 497.

(38) Several groups have attempted to model the surface of the various crystallographic faces of aluminas (in particular, transitional phases γ - or η -alumina having a defect spinel structure), among them Knözinger and Ratnasamy (see ref 37a) who have developed a model (still actively debated but nevertheless widely accepted in the literature) to describe the microstructure of O–H groups present on alumina. Up to five distinct bands (maximum number) can be observed on the infrared spectrum of a partially dehydroxylated γ -alumina, relative intensities of which depend on the nature of the exposed crystal faces, the degree of exposure of these faces, and the dehydroxylation temperature. According to the configuration that a OH group adopts, several types of OH groups have been distinguished, namely type I, which consists of terminal OH groups coordinated either to a single tetrahedral Al^{3+} cation (type Ia) or to a cation in an octahedral site (type Ib), type II, which describes bridging OH groups linked either to a tetrahedral and an octahedral cation (type IIa) or to two cations in octahedral positions (type IIb), and type III, in which the OH group is coordinated to three cations in octahedral interstices. The Brønsted acidities of these hydroxyls are different and decrease in the order $\text{III} > \text{IIa} > \text{IIb} > \text{Ia} > \text{Ib}$. At $500\text{ }^\circ\text{C}$, the global concentration of hydroxyl groups of the γ -alumina used here was estimated to be $4\text{ OH}/\text{nm}^2$.

(39) The infrared spectrum is available in the Supporting Information.

(40) (a) Pitzer, K. S.; Gutowsky, H. S. *J. Am. Chem. Soc.* **1946**, *68*, 2204. (b) Schram, E. P.; Hall, R. E.; Glone, J. D. *J. Am. Chem. Soc.* **1969**, *91*, 6643.

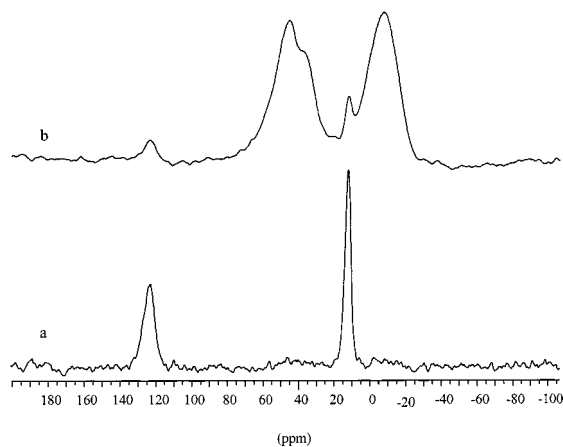
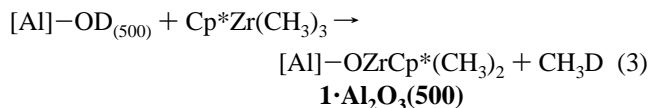


Figure 3. CP-MAS ^{13}C NMR spectra of (a) $1\cdot\text{Al}_2\text{O}_3(500)$ (Zr, 1.3 wt %) and (b) $1\cdot\text{Al}_2\text{O}_3(500)\text{-}^{13}\text{C}$ (Zr, 0.53 wt %).

methane- d_1 evolved during the grafting reaction was quantified by GC-MS and was found to be 0.85 mol of CH_3D /mol of grafted zirconium. The surface elemental analysis of the resulting solid gave a C/Zr molar ratio varying between 11.9 and 12.1.

In addition, deuterolysis of $1\cdot\text{Al}_2\text{O}_3(500)$ was performed to determine the number of methyl groups remaining on zirconium. Almost 2.1 mol of CH_3D /mol of grafted zirconium was liberated when $1\cdot\text{Al}_2\text{O}_3(500)$ was treated with heavy water at room temperature overnight.⁴¹ Carbon and zirconium analyses, after deuterolysis, gave a C/Zr molar ratio of 10.1.

These results have allowed us to determine that **1** has, at least initially, reacted with surface hydroxyl groups to form a complex that is σ -bonded to the surface via one covalent Zr-O-Al bond with liberation of 1 equiv of methane. The supported complex $1\cdot\text{Al}_2\text{O}_3(500)$ can thus be formulated as $[\text{Al}]_x\text{-O-Cp}^*\text{Zr}(\text{CH}_3)_2$, but its infrared spectrum, as well as other spectroscopic characteristics such as EXAFS (vide infra), suggests a variety of different local coordination environments.

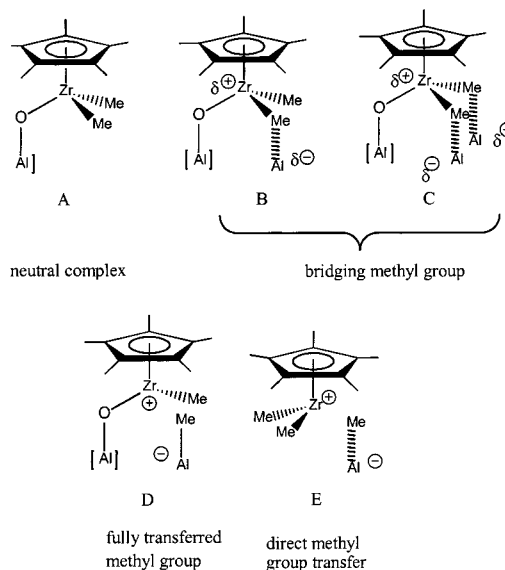


Further characterizations were achieved by solid-state ^1H , CP-MAS ^{13}C NMR, and EXAFS spectroscopy. In fact, the proton NMR did not supply information about the structures of the surface complexes.³⁰

(a) CP-MAS ^{13}C NMR. The CP-MAS ^{13}C NMR spectrum of the ^{13}C -enriched surface species, $1\cdot\text{Al}_2\text{O}_3(500)\text{-}^{13}\text{C}$ (Figure 3b), exhibited five signals of unequal intensity. The weak signals at 122 and 10 ppm are unambiguously assigned to the sp^2 and sp^3 carbons of the Cp^* ligand (carbon ring and methyl groups). The high-intensity signals at 42, 35, and -11 ppm correspond to the carbons of ^{13}C -enriched methyl groups, indicating the presence on the alumina surface of several species.⁴²

(41) The deuterolysis reaction was first followed by in situ infrared spectroscopy on the $\text{Cp}^*\text{Zr}(\text{CD}_3)_3/\text{Al}_2\text{O}_3(500)$ species. The supported complex was exposed to heavy water vapor (15 Torr) for several hours at room temperature. The bands characteristic of the Zr- CD_3 vibrations in the 2100-2000 cm^{-1} region disappeared totally on contact. At the same time, a broad band around 2750 cm^{-1} appeared, including probably the $\nu(\text{Zr-OD})$ vibration, the $\nu(\text{Al-OD})$ vibrations, isolated and associated by hydrogen bonds, and the vibrations assigned to physisorbed D_2O . No Cp^*D was detected in the gas phase. The conditions of complete reaction thus established, the deuterolysis was repeated on a larger scale with $1\cdot\text{Al}_2\text{O}_3(500)$ produced by the reaction between **1** and deuterated alumina.

Scheme 2



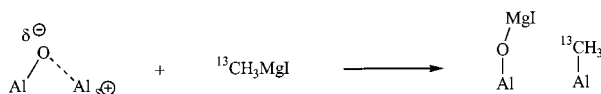
Before attempting to assign these different peaks, we should first discuss the different structures possible given the complexity of the alumina surface. A first group of structures would be the result of the reaction of **1** with the five different types of Al-OH groups present without secondary interactions with the surface. That is, initially we should expect five different neutral zirconium species having the formula $[\text{Al}]_x\text{-OZrCp}^*\text{Me}_2$ (the expression $[\text{Al}]_x$ refers to a surface alumina site which can involve one or more aluminum atoms together with one oxygen atom, Scheme 2, structure A). Since these species differ only in the geometry of the aluminum atom, we would expect that the chemical shift of the methyl groups would be very nearly the same, and thus we would expect in the CP-MAS NMR spectrum one broadened peak for all such structures. But as already mentioned, there are also coordinatively unsaturated aluminum Lewis acidic sites present at the alumina surface. If such sites were in close proximity to the initial $[\text{Al}]_x\text{-OZrCp}^*\text{Me}_2$ complex, we would expect an interaction with one or two zirconium methyl groups, involving the formation of either bridging methyl groups, $\text{Zr}-(\mu\text{-CH}_3)\text{-}[\text{Al}]_x$ (structures B and C), or full transfer of the methyl group to an aluminum vacancy, producing a true cationic zirconium species, $([\text{Al}]_x\text{-OZrCp}^*\text{Me})^+$, with real charge separation and a methyl aluminum fragment $[\text{Al-Me}]^-$ (structure D). We have represented also in Scheme 2 a true cationic zirconium complex, $[\text{Cp}^*\text{ZrMe}_2]^+$ (structure E), in which the methyl group has been transferred during the grafting reaction, with no covalent bond with the surface.

As previously mentioned, the ^{13}C NMR spectrum of $1\cdot\text{Al}_2\text{O}_3(500)\text{-}^{13}\text{C}$ (Figure 3b) exhibited three intense but very broad signals at 42, 35, and -11 ppm.⁴³ Given the simple spectrum of the silica-supported complex $1\cdot\text{SiO}_2(500)\text{-}^{13}\text{C}$, we assign the signal at 35 ppm to methyl groups bonded to a neutral zirconium atom (structure A).

(42) We performed studies, by CP MAS ^{13}C NMR, on the thermodecomposition and the decomposition under air of $1\cdot\text{Al}_2\text{O}_3(500)\text{-}^{13}\text{C}$ and concluded that the signals observed on the original spectrum were not due to decomposition products. During the thermodecomposition (from 25 to 120 $^\circ\text{C}$), the intensity of the signals at 42 and 35 ppm decreased without any appearance of other products on the surface. The decomposition under air leads to the formation of a new resonance at 58 ppm, probably due to the carbons of a Zr-OCH₃ group.

(43) As the spectra were recorded by using cross-polarization, the intensities are not directly related to the concentrations of the corresponding species, precluding any quantitative interpretation of the data.

Scheme 3



Concerning the signal at 42 ppm, it has been reported in the literature that the methyl group on a cationic or partially cationic zirconium complex appears at a slightly higher chemical shift than the corresponding neutral complex.^{7,11e,44} Thus, we tentatively assign this broad peak at 42 ppm to methyl groups on either “fully” or partially cationic zirconium species (structures B and D).

Although the NMR cannot exclude this formula, structure E was not retained, at least not as a major product. In the case of bicyclopentadienyl zirconium alkyl complexes supported on an alumina surface, some solid-state CP-MAS ¹³C NMR spectroscopic studies have been reported.^{11e,45} One of the possible pathways proposed to account for the reaction was the direct transfer of a methyl group of the precursor to surface Lewis acidic sites to produce [$>MO^-$][Cp₂Zr(¹³CH₃)⁺] and an [Al-¹³CH₃⁻] fragment. We cannot exclude this pathway, but taking into consideration (i) our infrared data showing full hydroxyls consumption, (ii) the quantity of methane-*d*₁ that evolved during the grafting reaction, and (iii) the quantity of deuterated methane produced by subsequent deuterolysis, the surface species produced by this pathway must be a minor product in our case, probably less than 10%.

The very large peak at -11 ppm can be assigned either to a bridging methyl group or to a methyl group that is fully transferred on an aluminum atom, (AlMe)⁻. To confirm this hypothesis, we reacted ¹³CH₃MgI with a totally dehydroxylated alumina (dehydroxylated at 1000 °C for 15 h under vacuum). The reaction likely proceeds by reaction with polarized Al-O-Al surface sites to produce an Al-¹³CH₃ fragment and an Al-O-MgI fragment (Scheme 3).

The CP-MAS ¹³C NMR spectrum of this product, which definitely has a terminal methyl group at aluminum, shows a peak at -9 ppm.

Nevertheless, a number of bridging methyl groups between zirconium and *alkyl* aluminum Lewis acids of molecular species have been reported, and their ¹³C NMR chemical shifts appear over a wide range of values depending on the substituents at zirconium and aluminum.^{36a,46} One still does not know where to expect a bridging methyl group between zirconium and an aluminum of the oxide surface.

Given the broadness (3100 Hz) of the peak at -11 ppm in the spectrum of **1**·Al₂O₃(500)-¹³C, one cannot determine with certainty by NMR alone either whether the peak is due to one or several species or whether the species in question involve bridging methyl groups or terminal methyl groups at aluminum. What is clear is that some interaction with surface aluminum is present.⁴⁷

(44) (a) Gillis, D. J.; Quyoum, R.; Tudoret, M.-J.; Wang, Q.; Jeremic, D.; Roszak, A. W.; Baird, M. C. *Organometallics* **1996**, *15*, 3600–3605. (b) Gillis, D. J.; Tudoret, M.-J.; Baird, M. C. *J. Am. Chem. Soc.* **1993**, *115*, 2543–2545.

(45) Dahmen, K. H.; Hedden, D.; Burwell, R. L.; Marks, T. J. *Langmuir* **1988**, *4*, 1212–1214.

(46) (a) Erker, G.; Albrecht, M.; Krüger, C.; Werner, S.; Binger, P.; Langhauser, F. *Organometallics* **1992**, *11*, 3517–3525. (b) Bochmann, M.; Sarsfield, M. J. *Organometallics* **1998**, *17*, 5908–5912. (c) Harlan, C. J.; Bott, S. G.; Barron, A. R. *J. Am. Chem. Soc.* **1995**, *117*, 6454–6474.

(47) We attempted also to confirm the presence of Al-¹³CH₃ fragments by MAS ²⁷Al NMR spectroscopy, but the peaks for tetrahedral and octahedral aluminum (at 63 and 7 ppm, respectively) were very broad, and we cannot draw any definitive conclusion from this technique.

Table 2. Zr K-Edge EXAFS-Derived Structural Parameters for **1**·Al₂O₃(500)^a

shell	coordination		<i>R</i> factor (%)	2σ ² (Å ²)
	number	distance (Å)		
O	0.9 (0.1)	2.01 (3)	29.6	0.028 (0.012)
C	1.8 (0.2)	2.18(2)		0.016 (0.004)
C	4.6 (0.5)	2.55 (1)		0.019 (0.002)
Al	2.9 (0.3)	3.21 (1)		0.022 (0.002)

^a For Zr K-edge spectra, AFAC = 0.8. *E*_f value for species **1**·Al₂O₃(500) is 0.36 eV. Debye–Waller factor σ-root-mean-square internuclear separation. The values given in parentheses represent the statistical errors generated in EXCURVE; for true estimation of errors see ref 52.

(b) EXAFS of **1**·Al₂O₃(500)-¹³C. Zr K-edge EXAFS measurements were performed on alumina(500)-supported zirconium species to improve our understanding of the surface species formed (Table 2 and Supporting Information). Analysis of the EXAFS data gave a first coordination sphere of about one oxygen at 2.01 Å and a second coordination sphere of about two carbons at 2.18 Å. Attempts to fit the EXAFS data using either a single shell of light scatterers (C or O) or other combinations of carbon and oxygen resulted in unacceptable fits, higher *R* factors, or unacceptably high Debye–Waller factors. Zr–C and Zr–O distances compare favorably with those found in Cp*Zr(IV) complexes, Cp*(CH₃)₂Zr(N(Si(CH₃)₃-(C₁₂H₁₇))) (average Zr–C 2.26 Å),⁴⁸ Cp*₂Zr(OH)₂ (average Zr–O 1.99 Å),⁴⁹ and Cp₂*Zr(OH)(O^tBuC=CH₂) (average Zr–O 2.01 Å).⁵⁰

Further support for this formulation is provided by the presence of additional backscattering shells due to about five carbons at 2.55 Å and about three aluminums at 3.21 Å. The shell at 2.55 Å can be assigned to the five carbons of the pentamethylcyclopentadienyl group and compares favorably with the distance expected for an average Zr–Cp* bond.⁵¹

The first and most significant result of this experiment is the finding of two methyl groups in the inner coordination sphere of zirconium. This would indicate that little or none of the surface complex derived by the reaction of **1** with hydroxyl groups, [Al]_x–OZrCp*Me₂, has fully transferred a methyl group to the alumina surface, leading to a separated ion pair due to the rigidity of the surface.

Moreover, the values obtained for the Zr–O and Zr–C are typical of covalent Zr–O and Zr–C bonds. This confirms that the ionic species (Scheme 2, structure E) held at the surface just by Coulombic interactions was at best a minor product.

The EXAFS data can be best fitted to a model containing three aluminum atoms in the vicinity of zirconium. Taking into account two methyl groups and a cyclopentadienyl ligand at zirconium and three aluminum atoms in the outer coordination sphere, and given the complexity of the structure of the γ-alumina surface, we can propose two main structures which are fully compatible with all the spectroscopic and analytical data.⁵³ The first one (Scheme 4, **a**) exhibits neutral character

(48) Shah, S. A. A.; Dorn, H.; Roesky, J. W.; Parsini, E.; Schmidt, H. G.; Noltemeyer, M. *J. Chem. Soc., Dalton Trans.* **1996**, *21*, 4143.

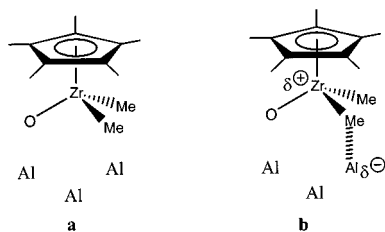
(49) Howard, W. A.; Parkin, G. *Polyhedron* **1993**, *12*, 1253.

(50) Howard, W. A.; Trmka, T. M.; Waters, M.; Parkin, G. *J. Organomet. Chem.* **1997**, *528*, 95.

(51) Fitting a further shell of about five carbons between 3.52 and 3.72 Å (to fit the CH₃ groups from the Cp* ring) did not lead to an improvement in the fit and instead produced higher *R* factors and higher Debye–Waller correlations.

(52) Corker, J. M.; Evans, J. *J. Chem. Soc., Chem. Commun.* **1994**, 1027. (b) Corker, J. M.; Evans, J.; Leach, H.; Levason, W. *J. Chem. Soc., Chem. Commun.* **1989**, 181.

Scheme 4



with two free methyl groups. The second one (Scheme 4, **b**) has a partially cationic character due to the interaction of one methyl group with a Lewis acidic aluminum site.

These results do not preclude the existence of smaller proportions of sites with one or two neighboring aluminum centers.

In conclusion, infrared observation of the reaction of Cp^*ZrMe_3 with the surface of $\gamma\text{-Al}_2\text{O}_3(500)$ leads to an irreversible reaction involving the consumption of all surface hydroxyl groups and the formation of a new surface complex, $\mathbf{1}\cdot\text{Al}_2\text{O}_3(\mathbf{500})$, having cyclopentadienyl and methyl ligands at zirconium. One equivalent of methane (per Zr) was evolved, suggesting a simple protonolysis grafting reaction. Elemental analysis is consistent with a general formula, $[\text{Al}]_x\text{-OZrCp}^*\text{Me}_2$. Carbon MAS NMR of an isotopically labeled analogue, $\mathbf{1}\cdot\text{Al}_2\text{O}_3(\mathbf{500})\text{-}^{13}\text{C}$, indicates that some of the surface complex has undergone further interaction with the alumina surface, either involving bridging methyl groups between zirconium and aluminum or involving full transfer of a methyl group. EXAFS experiments tend to favor the former (two carbons in the inner coordination sphere) and indicate that zirconium has three aluminum atoms in its outer coordination sphere: $[\text{Al}]_3\text{-OZrCp}^*(\text{CH}_3)_2$.

Niobia. Niobia is not often used as a support in surface organometallic chemistry. Some time ago, we reported the synthesis of a supported niobia methylrheniumtrioxo complex which was remarkably active for olefins metathesis reactions.⁵⁴ The high metathesis activity was correlated to the Lewis acidity of the support. Thus, niobia is studied here to further explore the effect of its surface Lewis acidity on polymerization catalysts. The surface acidity of niobia depends on the temperature of pretreatment. The highest number of Lewis acid sites is observed for a pretreatment temperature between 200 and 300 °C, whereas the number of Brønsted acid sites is higher at lower temperatures, e.g., 110 °C. We chose a $\text{Nb}_2\text{O}_5(300)$ for which the total amount of acidic sites (Lewis and Brønsted) remained constant (ca. 155×10^{-6} mol/g).⁵⁴

When **1** was sublimed onto a disk of $\text{Nb}_2\text{O}_5(300)$, the infrared spectrum showed that the very weak bands attributed to the $\nu(\text{Nb-OH})$ vibrations in the 3740–3680 cm^{-1} region disappeared totally on contact at room temperature with the zirconium complex. Simultaneously bands appeared in the regions 3100–2800 and 1500–1350 cm^{-1} , assigned to the $\nu(\text{C-H})$, $\nu(\text{C-C})$, and $\delta(\text{C-H})$ vibrations of the Cp^* ligand and methyl groups

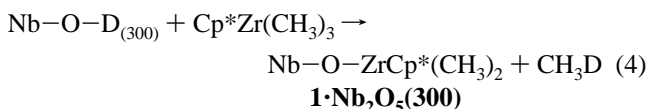
(53) The reason we do not propose a detailed drawing of the surface alumina structure is the complexity of the spinel structure of γ -alumina. There are tetrahedral Al's surrounded by O–Al linkages in which the second Al is either tetrahedral or octahedral. Additionally, there are some vacancies in the bulk structure. Consequently, we consider that it is not realistic to really propose such a mixture of species. In contrast, we believe that, on the alumina surface, under the influence of the zirconium complex and the oxophilicity of the zirconium, surface reconstruction occurs in which the grafted metal and its ligands change the surface geometry of the alumina surface.

(54) (a) Buffon, R.; Auroux, A.; Lefebvre, F.; Leconte, M.; Choplin, A.; Basset J.-M. *J. Mol. Catal.* **1992**, *76*, 287. (b) Buffon, R. Ph.D. Thesis, Université Claude Bernard, Lyon I, No. 202-92, 1992.

(Table 1). The color of the disk, initially gray, turned to brown during the reaction.

$\text{Cp}^*\text{Zr}(\text{CH}_3)_3$ which had not reacted was removed as mentioned above under vacuum at room temperature. The elemental analysis of the disk performed after the infrared experiments confirmed the presence of zirconium, but only small amounts were obtained (0.2–0.4 wt %). Methane was the only product that evolved during the course of the reaction.

The reaction was repeated on a larger scale with previously deuterated $\text{Nb}_2\text{O}_5(300)$. Almost 0.9 mol of CH_3D was liberated per grafted zirconium atom, indicating that the main reaction on the surface is a reaction with the OH groups. The elemental analyses of the obtained solid gave a molar C/Zr ratio of 11.7. Taken together, these results allowed us to propose a structure for $\mathbf{1}\cdot\text{Nb}_2\text{O}_5(\mathbf{300})$ in which the zirconium is monografted to the surface and bears in its coordination sphere one Cp^* ligand and two methyl groups, according to eq 4:



Further characterizations were performed, in particular CP-MAS ^{13}C NMR spectroscopy, but we failed to obtain a reliable ^{13}C NMR spectrum because of the low zirconium loading.

Discussion on the Reaction of $\text{Cp}^*\text{Zr}(\text{CH}_3)_3$ with Partially Dehydroxylated Oxides. Reaction of $\text{Cp}^*\text{Zr}(\text{CH}_3)_3$, **1**, with partially dehydroxylated silica, silica–alumina, alumina, and niobia is reported. **1** reacts with silica(500) by simple protonolysis of one Zr–Me bond by surface silanols, with formation of a unique, well-defined compound $[\equiv\text{Si-O-}]\text{ZrCp}^*(\text{CH}_3)_2$, $\mathbf{1}\cdot\text{SiO}_2(\mathbf{500})$. The complex exhibits a neutral character. **1** reacts with a silica–alumina(500) surface by a similar pathway, leading to a surface compound $\mathbf{1}\cdot\text{SiO}_2\text{-Al}_2\text{O}_3(\mathbf{500})$ with a chemical composition identical to that of $\mathbf{1}\cdot\text{SiO}_2(\mathbf{500})$. However, a fraction of $\mathbf{1}\cdot\text{SiO}_2\text{-Al}_2\text{O}_3(\mathbf{500})$ exhibits some interactions with aluminum Lewis centers via the methyl group coordinated to zirconium. **1** reacts also with the hydroxyl groups of a partially dehydroxylated γ -alumina, leading to a surface complex having also a chemical composition identical to those of $\mathbf{1}\cdot\text{SiO}_2(\mathbf{500})$ and $\mathbf{1}\cdot\text{SiO}_2\text{-Al}_2\text{O}_3(\mathbf{500})$: $[\text{Al}]_x\text{-OZrCp}^*(\text{CH}_3)_2$ (full disappearance of the Al–OH group in the infrared spectrum, liberation of 0.85 mol of CH_3D per grafted zirconium during the grafting reaction, liberation of 2.1 mol of CH_3D after deuteration of the grafted complex, satisfactory surface microanalysis (11.9 C/Zr, expected 12)). ^{13}C NMR gives more precise information on the real structure of the $\text{ZrCp}^*(\text{CH}_3)_2$ surface organometallic fragment. The Cp^* ligand exhibits the expected chemical shift. The methyl resonances are more complex than those for the silica-supported complex, suggesting at least three possible structures with no, partial, or full transfer of the methyl group to the Lewis acidic aluminum center, $[\text{Al}]_x\text{-OZrCp}^*(\text{CH}_3)_2$ (Scheme 2, A), $[\text{Al}]_x\text{-OZrCp}^*(\text{CH}_3)(\mu\text{-CH}_3\text{-}[\text{Al}]_x)$ (Scheme 2, B), $[[\text{Al}]_x\text{-OZrCp}^*(\text{CH}_3)^+][\text{Al-CH}_3^-]$ (Scheme 2, D). EXAFS data confirm the chemical composition of the grafted fragment ($\text{O-ZrCp}^*(\text{CH}_3)_2$) (Zr–O 2.01 Å, coordination number 1; Zr– C_{sp^3} 2.18 Å, coordination number 1.8; Zr– C_{sp^2} 2.55 Å, coordination number 4.6). The Zr–O distance (2.01 Å) is compatible with a covalent bond resulting from the protonolysis by Al–OH of a Zr–CH₃ bond. Moreover, the data cannot be fitted with a full transfer of a methyl to an aluminum center with formation of a rigid ion pair (Scheme 2, D). Interestingly, the EXAFS data at the Zr K-edge show three aluminums at a distance of 3.21 Å. Correlation between EXAFS and ^{13}C NMR data suggest, in

Table 3. Infrared Data and Assignments of the Molecular Complex $\text{Cp}_2\text{Zr}(\text{CH}_3)_2$, **2**, and of the Analogous Oxide-Supported Complexes

bands (values given in cm^{-1})	2		2·SiO₂(500)	2·SiO₂-Al₂O₃(500)	2·Al₂O₃(500)
	lit. ^a	exp ^b			
	3949		3949	3951	3946
$\nu(\text{C}-\text{H})_{\text{Cp}}$	3104	3103	3120	3117	3117
$\nu_{\text{as}}(\text{C}-\text{H})_{\text{Zr}-\text{CH}_3}$	2924	2925	2930	2936, 2926	2926
$\nu_{\text{s}}(\text{C}-\text{H})_{\text{Zr}-\text{CH}_3}$	2864	2868	2879	2878	2875
$2\delta_{\text{as}}(\text{C}-\text{H})_{\text{Zr}-\text{CH}_3}$	2778	2785	2799	2798	2798
harmonic bands	2729-1615	2723-1614	2730-1620	2730-1624	2730-1615
$\nu(\text{C}-\text{C})_{\text{E}_1 \text{ Cp}}$	1443	1444	1444	1443	1443
$\delta_{\text{as}}(\text{C}-\text{H})_{\text{Zr}-\text{CH}_3}$	1407	1414	1415	1417	1424
$\nu(\text{C}-\text{C})_{\text{E}_2 \text{ Cp}}$	1367	1369	1368	1368	1368
$\nu(\text{C}-\text{C})_{\text{A}_1 \text{ Cp}}$	1126				1126
$\text{Al}-\text{CH}_3$					1207

^a See ref 56. ^b Infrared spectrum in CCl_4 .

Table 4. Carbon Balance for Grafting Reactions of **2**

surface complexes	gaseous phase analysis, $\text{CH}_3\text{D}/\text{Zr}$ molar ratio ^a	surface microanalysis, C/Zr molar ratio ^a	mass balance, total C/Zr (expected 12)
2·SiO₂(500)	0.85	10.5	11.35
2·SiO₂-Al₂O₃(500)	1.1	10.3	11.4
2·Al₂O₃(500)	1	10.9	11.9

^a Average data obtained from several experiments.

short, two main surface structures: $[\text{Al}]_3-\text{OZrCp}^*(\text{CH}_3)_2$ and $[\text{Al}]_2-\text{OZrCp}^*(\text{CH}_3)(\mu-\text{CH}_3)-[\text{Al}]$.

I.B. Reaction of $\text{Cp}_2\text{Zr}(\text{CH}_3)_2$ with Partially Dehydroxylated Oxides. The same basic study was repeated using $\text{Cp}_2\text{Zr}(\text{CH}_3)_2$, **2**, as catalyst precursor, and in large part the interpretations of the results were very similar (assignment of IR and NMR spectra, etc.). Thus, the description of the study will be much less detailed than that given for **1**.

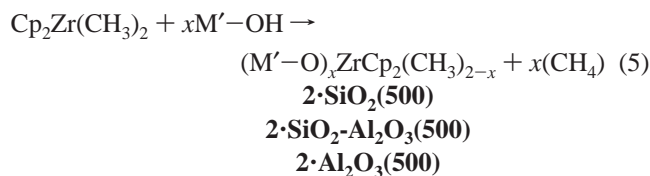
The reaction between $\text{Cp}_2\text{Zr}(\text{CH}_3)_2$, **2**, and the partially dehydroxylated oxides was followed by in situ infrared spectroscopy. The zirconium precursor was sublimed at 60 °C onto a disk (30 mg, at room temperature) of partially dehydroxylated (at 500 °C) silica, silica-alumina, and alumina. In the case of silica, no color change was observed, but for the other oxides ($\text{SiO}_2-\text{Al}_2\text{O}_3(500)$, $\text{Al}_2\text{O}_3(500)$) the white disk turned light yellow on reaction. In each infrared spectrum, the bands attributed to the surface hydroxyl groups in the 3900-3600 cm^{-1} region disappeared totally on contact at room temperature with the zirconium complex. At the same time, several bands appeared in the regions attributed to $\nu(\text{C}-\text{H})$, $\nu(\text{C}-\text{C})$, and $\delta(\text{C}-\text{H})$ vibrations of the Cp ligands and the Zr-methyl groups (3100-2700 and 1500-1150 cm^{-1}).

Methane was identified as the only gaseous product by gas chromatography. No liberation of cyclopentadiene was observed under the reaction conditions.⁵⁵ Excess **2** was easily removed by sublimation under vacuum at 60 °C. The infrared data of the obtained surface species and assignments are summarized in Table 3. Most of the vibrations had been identified by comparison with the infrared data of **2**.⁵⁶

Elemental analyses of the oxide disks confirmed the presence of zirconium (2-4 wt %). All these results suggest the formation of one or more chemisorbed zirconium species on the oxide surfaces according to eq 5.

(55) During the reaction, no cyclopentadiene was detected in the gas phase. To confirm that there was no cyclopentadiene physisorbed on the oxide, the solids were washed, after reaction, with small amounts of dry heptane. The heptane extracts were then analyzed by GC/MS, and no CpH was detected.

(56) See ref 25b.



To facilitate the quantification of methane and to perform reliable elemental analyses (C, Zr), we repeated the reactions on a larger scale (500 mg to 1 g) under a strict inert atmosphere. The reaction between **2** and the surface hydroxyl groups was reproduced using deuterated oxides. Nearly 1 mol of methane-*d*₁ was evolved per mole of grafted zirconium (0.85-1.1 mol of $\text{CH}_3\text{D}/\text{mol}$ of Zr) (Table 4), which confirms that a reaction has, indeed, taken place between the hydroxyl groups of the oxide surfaces and the molecular zirconium complex. These surface organometallic complexes were found to have a molar carbon/zirconium ratio varying between 10.3 and 10.9 (Table 4), which indicates that, on average, two Cp ligands and one methyl group per zirconium atom are left. Moreover, in the case of Cp_2ZrMe_2 grafted on alumina(500), the deuteration reaction of this surface organometallic species (carried out at room temperature overnight) liberated almost 0.8 mol of methane-*d*₁ per mole of grafted zirconium, thus confirming the presence of about one methyl group either at zirconium or at the neighboring aluminum center.

Further characterization of the surface species was accomplished by solid-state ¹H and CP-MAS ¹³C NMR spectroscopy and for **2·Al₂O₃(500)** also by EXAFS spectroscopy.

(a) ¹H NMR. The solid-state ¹H NMR spectra were determined for the different oxide-supported complexes as shown in Figure 4. The chemical shift data are summarized in Table 5.

In general, two types of signals, corresponding to the cyclopentadienyl ring protons and zirconium methyl group protons, were observed.⁵⁷ For the complex derived from silica, **2·SiO₂(500)**, the resonances were at 5.8 and -0.2 ppm ($\Delta\delta = 6.0$ ppm), whereas in the case of alumina peaks at 6.5 and 1.5 ppm ($\Delta\delta = 5.0$ ppm) were observed. It is not clear why there would be such a difference in the absolute chemical shift of the Cp protons, but perhaps it is due to differences in the bulk magnetic susceptibilities of the samples.⁵⁸ The difference in

(57) (a) Wailes, P. C.; Weigold, H.; Bell, A. P. *J. Organomet. Chem.* **1972**, *34*, 155. (b) Siedle, A. R.; Newmark, R. A.; Lamanna, W. M.; Schroepfer, J. N. *Polyhedron* **1990**, *9*, 301. (c) Borkowsky, S. L.; Jordan, R. F.; Hinch, G. D. *Organometallics* **1991**, *10*, 1268. (d) Lubben, T. V.; Wolcanski, P. T. *J. Am. Chem. Soc.* **1987**, *109*, 424. (e) Jordan, R. F.; Bajgur, C. S.; Dasher, W. E. *Organometallics* **1987**, *6*, 1041. (f) Jordan, R. F. *J. Organomet. Chem.* **1985**, *294*, 321-326.

(58) We did not use an internal reference because our samples are very sensitive and reactive.

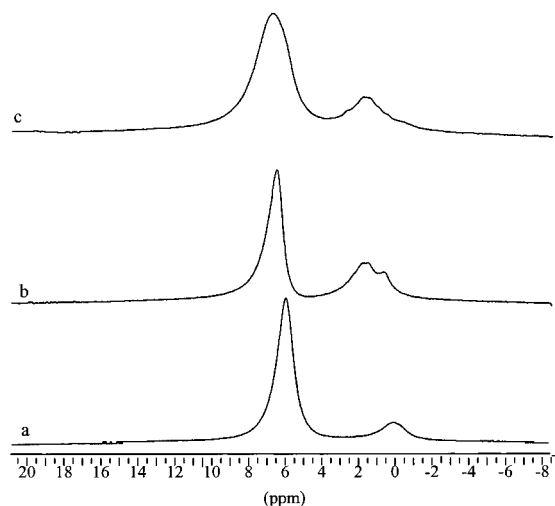


Figure 4. Solid-state ^1H NMR spectra of (a) $2\cdot\text{SiO}_2(500)$ (Zr, 3 wt %), (b) $2\cdot\text{SiO}_2\text{-Al}_2\text{O}_3(500)$ (Zr, 0.4 wt %), and (c) $2\cdot\text{Al}_2\text{O}_3(500)$ (Zr, 1.8 wt %).

Table 5. ^1H Chemical Shifts^a and Assignments

complexes	C_5H_5	CH_3
2	5.7	-0.12
2·SiO₂(500)	5.8	-0.2
2·SiO₂-Al₂O₃(500)	6.3	0.4, 1.3
2·Al₂O₃(500)	6.5	1.5

^a In ppm relative to tetramethylsilane (TMS).

chemical shifts ($\Delta\delta$) was thus used to identify the site to which the methyl group is bonded.

The ^1H NMR spectrum of the species supported on silica–alumina, $2\cdot\text{SiO}_2\text{-Al}_2\text{O}_3(500)$ (Figure 4b), exhibited three resonances at 6.3, 1.3, and 0.4 ppm. The downfield resonance was assigned to the cyclopentadienyl protons, whereas the upfield resonances were attributed to the protons of two different Zr–methyl groups. The methyl group corresponding to the signal at 1.3 ppm was close to that observed for the alumina-supported complex, $2\cdot\text{Al}_2\text{O}_3(500)$ ($\Delta\delta \approx 5.0$ ppm). The second methyl group at 0.4 ppm was similar to that seen for the silica-supported complex, $2\cdot\text{SiO}_2(500)$ ($\Delta\delta \approx 5.9$ ppm). Given the high silica percentage of the solid (SiO_2 75%, Al_2O_3 25%) and the fact that only $\equiv\text{Si-OH}$ hydroxyl groups were present at the surface before reaction, one would expect methyl signals similar to those observed for the silica-supported complex. Some of the surface species must, however, be in proximity to alumina sites on the surface, producing a chemical environment similar to that observed for alumina. We observed two methyl peaks only for solids with a low zirconium loading (0.4 wt %). When the solids contained more zirconium (>0.4 wt %), only one methyl group signal was observed with a $\Delta\delta$ of 6.0 ppm, as in the silica-supported complex.

(b) CP-MAS ^{13}C NMR. The ^{13}C CP-MAS NMR spectra of the surface species contained only one signal (attributed to the carbons of the cyclopentadienyl rings)^{57b–f} in the region 110–115 ppm. The carbons of the methyl groups bonded directly to the zirconium atom were not detected.

To better determine the nature of the methyl groups of these complexes by ^{13}C NMR, we undertook the synthesis of the isotopically enriched starting material $\text{Cp}_2\text{Zr}(^{13}\text{CH}_3)_2$, $2\text{-}^{13}\text{C}$. This compound was prepared according a procedure described in the literature and was characterized by solution- and solid-state ^{13}C NMR.⁵⁹ The reaction of $2\text{-}^{13}\text{C}$ with the various oxides was performed as previously described. The ^{13}C chemical shifts and assignments are summarized in Table 6.

Table 6. Solid-State ^{13}C NMR Chemical Shifts^a and Assignments

complexes	Cp–C	Zr–CH ₃	Al–CH ₃
2-^{13}C	114	33	
2·SiO₂(500)-^{13}C		22	
2·SiO₂-Al₂O₃(500)-^{13}C	111	22	
2·Al₂O₃(500)-^{13}C	115	30 (broad), 16	-12

^a In ppm relative to tetramethylsilane.

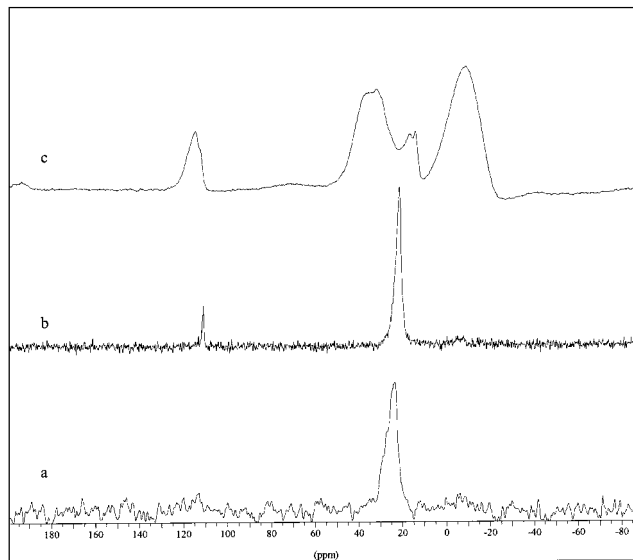


Figure 5. CP-MAS ^{13}C NMR spectrum of (a) $2\cdot\text{SiO}_2(500)$ (Zr, 3.0 wt %), (b) $2\cdot\text{SiO}_2\text{-Al}_2\text{O}_3(500)$ (Zr, 2.5 wt %), and (c) $2\cdot\text{Al}_2\text{O}_3(500)$ (Zr, 2.1 wt %).

A weak resonance (natural abundance ^{13}C) associated with the cyclopentadienyl ligands was observed for the surface complexes at approximately the same chemical shift, 111–115 ppm.⁶⁰ However, sharp differences in the methyl group region of the spectrum between the various supported complexes were noted.

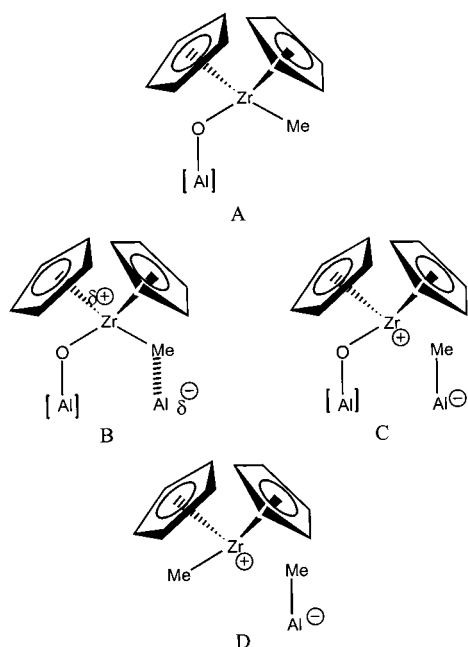
The spectrum of the silica- and silica–alumina-supported $\text{Cp}_2\text{Zr}(^{13}\text{CH}_3)_2$ exhibited only a single resonance (at 22 ppm) in the methyl group region (Figure 5a,b) which could be associated with the neutral zirconium species, $[\equiv\text{Si-O-ZrCp}_2\text{-Me}]$. The upfield displacement of this signal with respect to the precursor (33 ppm) is a consequence of the replacement of one methyl group by a surface siloxy group.^{57b,d,e} This replacement results in a more electron-rich zirconium due to π -donation of oxygen lone pairs. For example, the chemical shift of the two methyl groups of Cp_2ZrMe_2 is 30 ppm, whereas the chemical shift of the methyl group of $\text{Cp}_2\text{Zr(Me)(OMe)}$ is 19 ppm.

In the case of the alumina-supported species, $2\cdot\text{Al}_2\text{O}_3(500)\text{-}^{13}\text{C}$, we obtained a more complex ^{13}C NMR spectrum, which is, in fact, not surprising given the complexity of the alumina surface. One can observe in Figure 5c the presence of at least

(59) (a) Samuel, E.; Rausch, M. D. *J. Am. Chem. Soc.* **1973**, *95*, 6263–6267. (b) Hegedus, L.; Lipshutz, B.; Nozaki, H.; Reetz, M.; Rittmeyer P.; Smith, K.; Totter, F.; Yamamoto, H. In *Organometallics in Synthesis*; Schlosser, M., Ed.; John Wiley and Sons: New York, 1994. (c) Ortiz, B.; Barrios, H.; Walls, F. *Chem. Ind.* **1979**, 747. ^{13}C NMR: the solution-state proton-coupled ^{13}C NMR spectrum of $\text{Cp}_2\text{Zr}(^{13}\text{CH}_3)_2$, $2\text{-}^{13}\text{C}$, exhibited a doublet centered at 110.4 ppm ($^1J_{\text{CH}} = 172$ Hz), corresponding to the carbons of the cyclopentadienyl rings and a quartet centered at 30.3 ppm ($^1J_{\text{CH}} = 117$ Hz) assigned to the carbons of the Zr– $^{13}\text{CH}_3$ groups. The solid-state CP-MAS ^{13}C NMR spectrum of $2\text{-}^{13}\text{C}$ was characterized by a single intense signal at 33 ppm, corresponding to the isotopically labeled Zr–methyl groups and its spinning sidebands ($\delta \pm 2700$ Hz).

(60) The carbons of the Cp ligand are not seen in the spectrum of $2\cdot\text{SiO}_2(500)$ because the number of scans was not sufficient to distinguish this signal.

Scheme 5



three types of ^{13}C -enriched methyl groups around 30, 16, and -12 ppm. Before attempting to assign these different peaks, we have to review the various structures which could exist on the alumina surface.

A first group of structures, formulated as $[\text{Al}]_x\text{-OZrCp}_2\text{Me}$ (Scheme 5, A), has been considered. They would be the result of the reaction of Cp_2ZrMe_2 with the different types of Al–OH groups present on alumina(500). The surface zirconium species would not undergo any secondary reactions with the surface and would present, therefore, a neutral character.

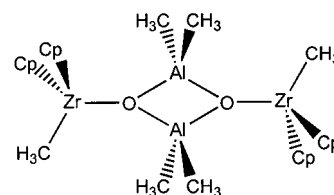
A second group of structures may take into account Lewis acid centers of alumina. If Lewis acidic sites of the surface are close enough to the initial $[\text{Al}]_x\text{-OZrCp}_2\text{Me}$ complex, we would expect interactions with the remaining methyl group, which could bridge between a zirconium and an aluminum atom, $\text{Zr}-(\mu\text{-Me})\text{-}[\text{Al}]_x$ (Scheme 5, B) or be totally transferred to the aluminum center, producing a true cationic zirconium species without any methyl group left on zirconium, $[\text{Al}]_x\text{-OZrCp}_2^+$, and an Al–Me fragment (Scheme 5, C).

The last structure involves the direct transfer of a methyl group of Cp_2ZrMe_2 to surface Lewis acidic sites. This pathway, proposed by Marks,^{11e} would lead to the formation of a “cation-like” zirconium species, $[[\text{Al}]_x\text{-O}^-][\text{Cp}_2\text{Zr}(\text{Me})^+]$ (Scheme 5, D), linked to the surface via Coulombic interactions and the concomitant formation of an Al–Me fragment.

Let us try to assign the different NMR chemical shifts to one or several of the proposed structures. The chemical shifts of methyl groups in several molecular complexes of the type $\text{Cp}_2\text{ZrCH}_3(\text{OR})$ are extremely helpful.^{57c,e} In particular, the dimer $[\text{Cp}_2\text{Zr}(\text{Me})(\text{OAlMe}_2)]_2$, **3**,⁶¹ has one covalent Zr–O bond, two cyclopentadienyl ligands, one methyl coordinated to zirconium, and two aluminums linked to the oxygen (Scheme 6). We shall see later by EXAFS that the crystallographic distances as well as the first and the second coordination spheres of zirconium are similar. It is therefore expected that ^{13}C NMR chemical shift of this model should be useful for interpretation. Indeed, the Zr–Me and Al–Me resonances of this molecular dimer are situated respectively at 28.4 and -5.9 ppm. We can

(61) Erker, G.; Albrecht, M.; Werner, S.; Krüger, C. *Z. Naturforsch., Teil B* **1990**, *45*, 1205.

Scheme 6



therefore assign the 30 ppm resonance to a neutral Zr–Me species (Scheme 5, A). This signal is, however, very broad (3401 Hz), and one could imagine that it represents a mixture of surface species: structural isomers of species A,⁶² and chemically different species such as species D.⁶³ Such cationic species D may exist in our case, but, taking into consideration the infrared experiments (consumption of all the Al–OH groups) and the fact that 1 equiv of methane was given off during the grafting reaction, species D cannot be the only component of the peak that we observed around 30 ppm and must probably be present in small amounts (*vide infra*).

By comparison with the chemical shifts reported for some alkyl aluminum compounds,^{17c,36a,64} we attribute the upfield signal at -12 ppm to Al– ^{13}C entities (either terminal or bridged). The width of this signal (2718 Hz), probably due to the quadrupolar aluminum nucleus, is consistent with this assignment. This broadness may also be due to different sites. These entities could be formed by the complete or partial transfer of a methyl group to an aluminum vacant site of the surface. The complete transfer could have taken place during the grafting, producing species D, or after the grafting in a secondary reaction, producing species C.

The weak signal at 16 ppm is situated between the regions generally associated with Zr–methyl groups ($\delta \approx 30$ ppm) and Al–methyl groups ($\delta \approx -10$ ppm) and cannot be assigned reliably to a structure.

(c) EXAFS Spectroscopy of $2 \cdot \text{Al}_2\text{O}_3(500)$. Analysis of the Zr K-edge EXAFS of the supported species $2 \cdot \text{Al}_2\text{O}_3(500)$ (Table 7 and Supporting Information) gave a best fit of a first coordination sphere of one oxygen at an average distance of 1.98 Å and a second coordination sphere of one carbon at 2.18 Å. This is consistent with the presence of one methyl and one surface oxygen bond. Previous EXAFS studies have shown typical Zr–O distances for Zr complexes supported on silica via σ -bonded surface $\equiv\text{Si}\text{-O}$ groups to be of the order of 1.96 Å.⁶⁵

Further support for this model is provided by the presence of an additional shell of carbons at 2.58 Å and a further coordination sphere at 3.40 Å. The shell at 2.58 Å can be assigned to the cyclopentadienyl group attached to the zirconium, and the further backscattering shell is due to the aluminums from the alumina surface, which gives further support for the model presented. It was found that splitting the short-distance shell into two shells due to the surface oxygen and the methyl group produced a considerably better *R* factor (10% reduction) and more acceptable correlations between the

(62) One must remember that a partially dehydroxylated alumina has several types of surface hydroxyl groups due to different combinations of aluminum geometries (T_d and O_h aluminums, and combinations thereof).

(63) On the basis of the appearance of a methyl group at 36 ppm in the solid-state ^{13}C NMR, Marks has proposed for the reaction of $\text{Cp}_2\text{Zr}(\text{CH}_3)_2$ with a partially dehydroxylated γ -alumina (PDA) the formation of some “cation-like” zirconium species, $[\text{Cp}_2\text{Zr}(\text{CH}_3)^+][\text{Al}(\text{CH}_3)^-]$ (see ref 11e).

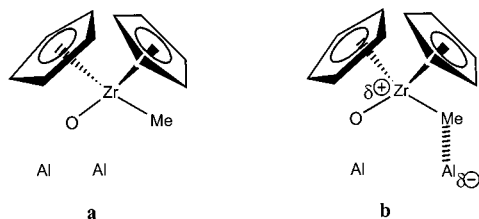
(64) (a) Kaminsky, W.; Luker, H. *Makromol. Chem. Rapid Commun.* **1984**, *5*, 225–228. (b) Kaminsky, W.; Miri, M.; Sinn, H.; Woldt, R. *Makromol. Chem. Rapid Commun.* **1983**, *4*, 417–421.

(65) Corker, J. M.; Lefebvre, F.; Lecuyer, C.; Dufaud, V.; Quignard, F.; Choplin, A.; Evans, J.; Basset, J.-M. *Science* **1996**, *271*, 966.

Table 7. Zr K-Edge EXAFS-Derived Structural Parameters for $2 \cdot \text{Al}_2\text{O}_3(\mathbf{500})^a$ and for the Molecular $[\text{Cp}_2\text{Zr}(\text{Me})(\text{OAlMe}_2)]_2$ Complex, **3** (see Ref 61)

	shell	coordination number	distance (Å)	R factor (%) $2 \cdot \text{Al}_2\text{O}_3(\mathbf{500})$	$2\sigma^2$ (Å ²)
$2 \cdot \text{Al}_2\text{O}_3(\mathbf{500})$ 3	O	1.0 (0.1)	1.98 (2)	25.3	0.022 (0.007)
		1	2.044		
$2 \cdot \text{Al}_2\text{O}_3(\mathbf{500})$ 3	C	1.0 (0.1)	2.18 (1)		0.005 (0.004)
		1	2.270		
$2 \cdot \text{Al}_2\text{O}_3(\mathbf{500})$ 3	C	8.8 (0.5)	2.58 (1)		0.019 (0.002)
		10	2.507		
$2 \cdot \text{Al}_2\text{O}_3(\mathbf{500})$ 3	Al	2.0	3.40 (1)		0.020 (0.004)
		2	3.57		

^a For Zr K-edge spectra, AFAC (0.3) = 0.8. E_f value for species $2 \cdot \text{Al}_2\text{O}_3(\mathbf{500})$ is -3.61 eV. Debye–Waller factor σ -root-mean-square internuclear separation. The values given in parentheses represent the statistical errors generated in EXCURVE; for true estimation of errors see ref 52.

Scheme 7

interatomic distances and Debye–Waller factors. The EXAFS-derived average Zr–C distances due to the cyclopentadienyl group (2.58 Å) compare favorably with those found in the biscyclopentadienyl Zr(IV) complexes, $[\text{Cp}_2(\text{CH}_3)\text{ZrOAl}(\text{CH}_3)_2]_2$ (2.51 Å average),⁶¹ $[\text{Cp}_2(\text{CH}_3)\text{Zr}]_2\text{O}$ (2.54 Å average),⁶⁶ and $\text{Cp}_2(\text{CH}_3)\text{ZrO}(\text{CH}_3)(\text{C}=\text{C})(\text{C}_6\text{H}_5)_2$ (2.53 Å average).⁶⁷ The EXAFS data for Zr–Al backscattering could also be best fitted to a model containing two aluminum atoms.

The first significant result of this experiment is the finding of one methyl in the inner coordination sphere of zirconium. This indicates that species C, derived by the reaction with hydroxyl groups followed by the complete transfer of the remaining methyl group to the alumina surface, could be present as a minor species. Moreover, the values obtained for the Zr–O and Zr–C distances compare favorably with those found for covalent Zr–O and Zr–C bonds of molecular analogues (Table 7). The distance Zr–O of 1.98 Å rules out the possibility of the existence of species D, which is bound to the surface via ionic interactions. If present, it should exist in very small amounts.

So, taking into account one methyl group, one oxygen atom, two cyclopentadienyl ligands at zirconium, and two aluminum atoms in the outer coordination sphere, two main structures can be proposed (Scheme 7). The first structure (a) would involve a zirconium which has reacted with alumina hydroxyl groups without further interactions with the surface. The second one (b) would result from an initial reaction with alumina hydroxyl groups in which the remaining methyl group is bridging to neighboring aluminum centers. Notice that the monocyclopentadienyl zirconium species has three and not two aluminum atoms in its coordination sphere. Perhaps the steric bulkiness of the two cyclopentadienyl ligands can prevent the zirconium from approaching the surface sufficiently to “see” more than two exposed aluminum atoms.

Discussion on the Reaction of $\text{Cp}_2\text{Zr}(\text{CH}_3)_2$ with Partially Dehydroxylated Oxides. Several important observations can be made for the grafting reaction of $\text{Cp}_2\text{Zr}(\text{CH}_3)_2$ with partially

dehydroxylated oxides. In all cases, during the grafting reaction about 1 equiv of methane- d_1 was liberated per equivalent of grafted zirconium, with the concomitant formation of chemisorbed surface zirconium species. The infrared experiments indicate also the total consumption of the surface hydroxyl groups on contact with the zirconium precursor. The main reaction which takes place on the surfaces is a reaction between one zirconium–methyl and one surface hydroxyl group: The resulting zirconium species are at least linked to the surface via one covalent M–O–Zr bond. Moreover, on the basis of elemental analyses, we can ascribe for the supported zirconium species a general structure of the type, $[\text{M}–\text{O}–\text{ZrCp}_2(\text{CH}_3)]$, where the zirconium atom is surrounded by two Cp ligands and one methyl group. Solid-state NMR spectroscopy, in particular with an isotopically labeled molecular precursor, provides detailed information concerning the structures of the surface organometallic complex.

In the case of silica–alumina (at least in the case of samples with high zirconium loading), all the results indicate that a single zirconium complex, $[\equiv\text{SiO}–\text{ZrCp}_2\text{Me}]$, is formed. Nevertheless, for silica–alumina we cannot rule out the possibility that the initially formed species interacts with neighboring Lewis acidic aluminum sites (see ¹H NMR, Figure 4b), depending on the zirconium loading of the sample.

In the case of the partially dehydroxylated alumina-supported species, the main reaction which takes place is also a simple protonolysis of one Zr–methyl bond by the surface hydroxyls. The global ratio of two cyclopentadienyls and one methyl group per zirconium is maintained, but the bonding of the methyl group is more difficult to evaluate. The solid-state ¹³C NMR spectra indicate the presence of a mixture of species having very different methyl group environments. Various structures, some clearly identified, others more speculative, have been proposed (Scheme 5). On the basis of ¹³C NMR spectrum, the formation of a neutral supported complex, $[\text{Al}]_x–\text{OZrCp}_2\text{Me}$ (Scheme 5, A) occurs by simple reaction of a surface hydroxyl with the precursor. Other species can be formed by partial or full transfer of the remaining methyl group to neighboring aluminum vacant sites, as indicated in Scheme 5, B and C. If the transfer were total, the cationic zirconium center would no longer bear an alkyl group and thus should not be active for the polymerization of olefins.

Marks has proposed several species for the same reaction, including an active species (Scheme 5, D) wherein there is no covalent link between zirconium and the surface. The elemental analysis of the surface complex, the amount of methane evolved during the grafting, and deuteration after grafting, together with the infrared experiments, tend to favor species A, B, and C in Scheme 5. Species D (formed without liberation of methane and consumption of hydroxyls), if present, should exist only in

(66) Hunter, W. E.; Hrnecir, D. C.; Bynum, R. V.; Penttila, R. A.; Atwood, J. L. *Organometallics* **1983**, *2*, 750.

(67) Gambarotta, W. E.; Strologo, S.; Floriani, C.; Chiesi-Villa, A.; Guatini, C. *Inorg. Chem.* **1985**, *24*, 654.

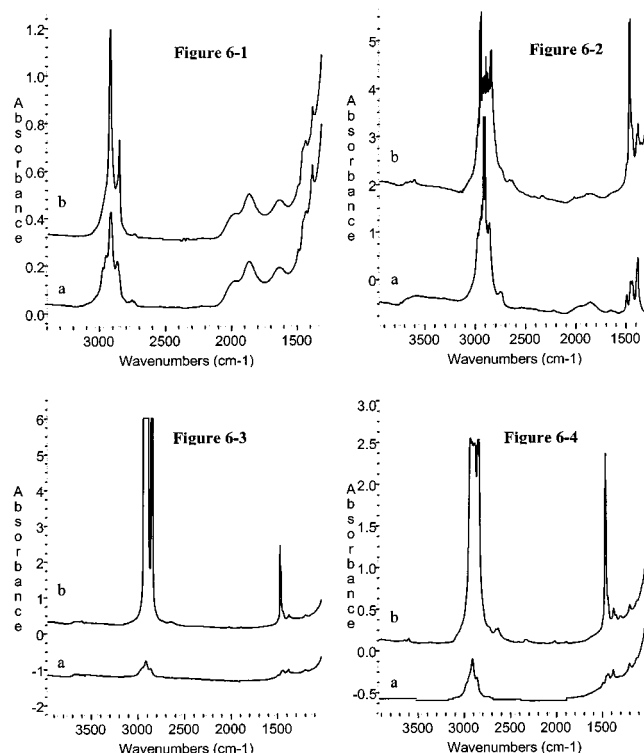


Figure 6. Infrared spectra of **1**·oxide(500): (a) (6-1, **1**·SiO₂(500); 6-2, **1**·SiO₂-Al₂O₃(500); 6-3, **1**·Al₂O₃(500); 6-4, **1**·Al₂O₃(1000)); (b) (a) + ethylene (200 Torr), 1 day, room temperature.

very small quantities. EXAFS results provide an even more detailed picture of the structures present on the surface. The finding of one methyl group and one oxygen atom at zirconium with covalently bonded Zr-C and Zr-O distances confirms that species D is a minor product in the reaction of Cp₂ZrMe₂ with Al₂O₃(500) and indicates that species C is also absent or is present as a very minor product. The total transfer of a methyl group from the zirconium to a Lewis acidic site of the surface seems not to be favored either during the grafting reaction or in a secondary reaction once the zirconium complex has been bound to the surface.

Given the results of two aluminum atoms in the outer sphere of zirconium, two structures can be proposed in Scheme 7. These two structures, [Al]₂-OZrCp₂CH₃ and [Al]-OZrCp₂(μ-CH₃-[Al]), can be considered as the major products of the reaction between Cp₂ZrMe₂ and Al₂O₃(500).

II. Ethylene Polymerization by Oxide-Supported Cyclopentadienyl Zirconium Alkyl Complexes. II.A. Preliminary Infrared Experiments for Catalytic Screening of the Various Surface Complexes. The reaction of ethylene with the supported complexes was followed by in situ infrared spectroscopy both on the surface and in the gas phase. The surface species, once synthesized, were exposed to a low pressure of ethylene (200 Torr) introduced in the IR cell through a deoxo/molecular sieves trap.

Rate of Formation of Adsorbed Polyethylene Followed by Infrared Spectroscopy. The catalytic activity of Cp*Zr(CH₃)₃ grafted on partially dehydroxylated silica, silica-alumina, and alumina and totally dehydroxylated alumina (Al₂O₃(1000)) toward ethylene polymerization had been studied by following the appearance of ν(C-H) vibrations of polyethylene in the region 3000–2800 cm⁻¹. The infrared spectra obtained for the various surface species before and after polymerization reaction are shown in Figure 6.

Table 8. Initial Activity of Supported Monocyclopentadienyl (Cp*Zr(CH₃)₃, **1**) and Biscyclopentadienyl (Cp₂Zr(CH₃)₂, **2**) Zirconium Complexes

complexes	activity (g PE mol ⁻¹ Zr atm ⁻¹ h ⁻¹)
1 ·SiO ₂ (500)	0
1 ·SiO ₂ -Al ₂ O ₃ (500)	0
1 ·Al ₂ O ₃ (500)	20 000
1 ·Al ₂ O ₃ (1000)	13 000
2 ·SiO ₂ (500)	0
2 ·SiO ₂ -Al ₂ O ₃ (500)	0
2 ·Al ₂ O ₃ (500)	3 000
2 ·Al ₂ O ₃ (1000)	0

In Figure 6-1, spectrum a, one can see the bands characteristic of **1**·SiO₂(500) whose chemical formula was determined as (≡SiO)ZrCp*(CH₃)₂. After 1 day of exposure to an ethylene pressure (200 Torr), new bands typical of a -(CH₂-CH₂)-_n fragment appeared at 2970, 2850, and 1380 cm⁻¹ (Figure 6-1, spectrum b).⁶⁸ The rather weak intensity of these bands suggests that only a few monomers have inserted in the Zr-methyl bonds of the surface species. This behavior on a neutral species is not surprising, since the active site in metallocene polymerization is supposed to be a cationic species.

In the case of Lewis acidic supports such as silica-alumina and alumina (Figure 6-2, 6-3, 6-4, spectra b), intense bands were formed at 2970, 2850, and 1380 cm⁻¹, corresponding respectively to the ν(C-H) and δ(C-H) vibrations of polyethylene. This indicates, as expected, a high activity for the supported species presenting some "cation-like" character.

The same trend was observed with the biscyclopentadienyl zirconium surface complexes: the silica-supported species did not insert any molecules of ethylene, whereas formation of polyethylene was observed for silica-alumina- and alumina-supported complexes.⁶⁹

Rate of Ethylene Consumption Followed by Infrared Spectroscopy. To obtain a first estimation of the activity of these catalysts toward ethylene polymerization, the polymerization was carried out in an infrared cell containing a larger quantity (100 mg) of powdered catalyst.

The infrared cell was aligned in the IR spectrometer so that the beam sampled only the gas phase above the solid. The disappearance of ethylene was evaluated by performing an integration over the entire ν(C-H) spectral region, 3100–2700 cm⁻¹, of the ethylene in the gas phase. The reactions were performed at 19 °C (the temperature was maintained constant), and the reactor was initially charged with 200 Torr of dry ethylene. The initial time, *t*₀, was determined when the seal separating the catalyst from the ethylene gas was broken.

Several experiments were carried out, under these conditions, with all of the complexes described above and with the alumina-(1000)-supported Cp*Zr(CH₃)₃ and Cp₂Zr(CH₃)₂, respectively **1**·Al₂O₃(1000) and **2**·Al₂O₃(1000). For the following complexes, little or no activity was observed: **1**·SiO₂(500), **2**·SiO₂(500), **1**·SiO₂-Al₂O₃(500), **2**·SiO₂-Al₂O₃(500), and **2**·Al₂O₃(1000) (Table 8).

Only three alumina-supported complexes, **1**·Al₂O₃(500), **1**·Al₂O₃(1000), and **2**·Al₂O₃(500), exhibited sufficient activity in ethylene polymerization, but their activity decreased dramatically with time (Table 8 and Supporting Information). Several

(68) For polyethylene infrared data, see: Pouchert, C. *The Aldrich Library of Infrared Spectra*, 3rd ed.; Aldrich Chemical Co.: Milwaukee, WI, 1981.

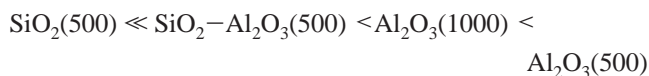
(69) The infrared spectra of the oxide-supported biscyclopentadienyl zirconium species before and after polymerization of ethylene are given in the Supporting Information.

factors may explain this phenomenon: decrease of the concentration of ethylene in the gas phase and, as the polymerization proceeds, inaccessibility of the active sites covered by the resulting polyethylene and/or unfavorable mass transfer of ethylene to the active site under our conditions.

In the case of the monocyclopentadienyl complexes, the initial activity was higher for **1**·Al₂O₃(500) than for **1**·Al₂O₃(1000) (Table 8). The same phenomenon occurs for the biscyclopentadienyl complexes, but the activity was generally much lower than for the supported monocyclopentadienyl species.

A few years ago, Marks et al. reported a better activity in ethylene polymerization for Cp₂Zr(CH₃)₂ grafted on a γ -alumina totally dehydroxylated (900 °C, DA) than for that grafted on a partially dehydroxylated one (450 °C, PDA).^{11e} These authors evoked the presence on Al₂O₃(900) of a cationic zirconium species, [Cp₂Zr(CH₃)]⁺[Al-CH₃]⁻, which could be responsible for the catalytic activity. On Al₂O₃(450), neutral “ μ -oxo zirconium alkyl species” were reported to be predominant, but they were considered to be inactive. In contrast to Marks, we proposed that some of the neutral “ μ -oxo zirconium species”, the main surface products on PDA, can also present a “cation-like” character (partially or totally cationic), leading to active species (vide supra). If we take our catalytic results into consideration, these active species would be more numerous on Al₂O₃(450) than on Al₂O₃(900).

To summarize, we have observed that in the mono- and the biscyclopentadienyl series, the activity in ethylene polymerization was strongly dependent on the nature of the oxide and the thermal treatment of the support according to the following order:



with Cp*Zr(CH₃)₃ > Cp₂Zr(CH₃)₂.

The most promising catalyst for ethylene polymerization was found to be **1**·Al₂O₃(500), and a more detailed study was undertaken to evaluate its activity in more realistic conditions. For comparison, the same study was carried out with **1**·SiO₂(500).

II.B. Kinetic Studies in Batch System. The catalysts obtained by reaction of Cp*ZrMe₃ with silica and alumina were tested in the polymerization of ethylene under various conditions. The first experiments were carried out without cocatalysts in order to evaluate their intrinsic activity. The behavior of these supported complexes was then studied in the presence of two different cocatalysts, MAO and B(C₆F₅)₃. For comparison, the activity of homogeneous catalysts (Cp*ZrCl₃, **1**′, Cp*ZrMe₃, **1**, Cp₂ZrCl₂, **2**′, and Cp₂ZrMe₂, **2**) was also determined under the same experimental conditions.

Ethylene Polymerization with Homogeneous Catalysts. We show in Table 9 the activities obtained for homogeneous mono- and biscyclopentadienyl catalysts associated with MAO or B(C₆F₅)₃. In general, whatever the cocatalyst used, the activities of the bisCp complexes were found to be the highest, about twice those of the monoCp* analogues. The same trend was previously reported in the literature.^{14b,70} We also observed a similar activity whether the precursor was a halogen or an alkyl complex (run 1 vs 2, run 4 vs 5). In the case of **1**, no activity was shown with B(C₆F₅)₃ in our conditions (run 3), which might suggest that the active species was either not formed in the reaction medium or not sufficiently stabilized by the noncoor-

(70) (a) Chien, J. C.; Wang, B.-P. *J. Polym. Sci., Polym. Chem.* **1990**, *28*, 15–38.

Table 9. Polymerization of Ethylene with Homogeneous Catalysts^a

run	catalyst	cocatalyst	maximum activity (kg PE mol ⁻¹ Zr h ⁻¹)	productivity (kg PE mol ⁻¹ Zr h ⁻¹)
1	Cp*ZrCl ₃ , 1 ′	MAO	3.5 × 10 ³	2.3 × 10 ³
2	Cp*ZrMe ₃ , 1	MAO	4 × 10 ³	3.2 × 10 ³
3	Cp*ZrMe ₃ , 1	B(C ₆ F ₅) ₃	0	0
4	Cp ₂ ZrCl ₂ , 2 ′	MAO	11 × 10 ³	8.7 × 10 ³
5	Cp ₂ ZrMe ₂ , 2	MAO	10 × 10 ³	7.7 × 10 ³
6	Cp ₂ ZrMe ₂ , 2	B(C ₆ F ₅) ₃	9.7 × 10 ³	3.6 × 10 ³

^a Polymerization conditions: 50 °C, 4 bar, 1 h, heptane (300 mL), [Zr] = 3 × 10⁻⁶ mol/L. MAO assays, [Al]/[Zr] = 500; B(C₆F₅)₃ assays, [B]/[Zr] = 1 with 0.5 mmol/L of TiBA as scavenger.

inated anion. Before now, a few cationic monoCp zirconium complexes activated with B(C₆F₅)₃ have been isolated, all of which were stabilized by the presence of arenes or phosphines in the zirconium coordination sphere.⁷¹

In contrast to Cp*ZrMe₃, Cp₂ZrMe₂ exhibited good activity in ethylene polymerization in the presence of B(C₆F₅)₃. The initial activity was similar to that obtained with MAO. After 1 h of reaction, we observed that the productivity was higher in the case of MAO (runs 5 and 6), indicating that the systems, when associated with B(C₆F₅)₃, deactivated more rapidly. It is well known that the role of MAO is not only the formation and/or the stabilization of the cationic species but also the regeneration of the active site during the polymerization.^{2f}

Ethylene Polymerization with Silica-Supported Monocyclopentadienyl Zirconium Catalysts. The activity of (≡SiO)-ZrCp*Me₂ was first evaluated in the absence of cocatalyst. This surface complex exhibited no catalytic activity (Table 10, run 8) under these conditions, which is consistent with our expectations given the neutral structure of the silica-supported species. Interestingly, **1**·SiO₂(500) can be activated by the introduction of a cocatalyst such as MAO or B(C₆F₅)₃ (respectively runs 9 and 10). In both cases, the activity was found to be lower than that for the corresponding homogeneous Cp*ZrMe₃ catalyst. For example, Cp*ZrMe₃ supported on silica activated with MAO was 14 times less active than the molecular Cp*ZrMe₃ activated also by MAO (run 9 vs 2).

As mentioned above for homogeneous complexes (Table 9, run 1 vs 2; run 4 vs 5) no noticeable changes in activity were detected when working with silica-supported chloride or alkyl zirconium complexes. The activity of the system **1**·SiO₂(500) activated with MAO (Table 10, run 9) was roughly of the same order as that reported in this work (Table 10, runs 7) and in the literature^{14b} for the system **1**′·SiO₂(500) activated also with MAO.

With borane systems, two methods were employed to activate the silica-supported monoCp* zirconium complex: (i) initial synthesis of the borane surface species by reacting (≡Si-O)-ZrCp*Me₂ with 1 equiv of B(C₆F₅)₃ in pentane at room temperature for 1 h, followed by the isolation of the resulting product, **1**·SiO₂(500)/B(C₆F₅)₃; (ii) in situ synthesis of the

(71) (a) Gillis, D. J.; Tudoret, M.-J.; Baird, M. C. *J. Am. Chem. Soc.* **1993**, *115*, 2543–2545. (b) Gillis, D. J.; Quyoum, R.; Tudoret, M.-J.; Wang, Q.; Jeremic, D.; Roszak, A. W.; Baird, M. C. *Organometallics* **1996**, *15*, 3600–3605. (c) Wang, Q.; Quyoum, R.; Gillis, D. J.; Tudoret, M.-J.; Jeremic, D.; Hunter, B. K.; Baird, M. C. *Organometallics* **1996**, *15*, 693–703. (d) Pellicchia, C.; Immirzi, A.; Grassi, A.; Zambelli, A. *Organometallics* **1993**, *12*, 4473–4478. (e) Pellicchia, C.; Longio, P.; Proto, A.; Zambelli, A. *Makromol. Chem., Rapid Commun.* **1992**, *13*, 265–268. (f) Amor, J. I.; Cuenca, T.; Gomez-Sal, P.; Manzanero, A.; Royo, P. *J. Organomet. Chem.* **1997**, *535*, 155–168. (g) Lancaster, S. J.; Robinson, O. B.; Bocchman, M.; Coles, S. J.; Hursthouse, M. B. *Organometallics* **1995**, *14*, 2456–2462.

Table 10. Polymerization of Ethylene with Supported **1·SiO₂(500)** and **1'·SiO₂(500)** Catalysts^a

run	catalyst	Zr (%wt)	cocatalyst	maximum activity (kg of PE mol ⁻¹ of Zr h ⁻¹)	productivity (kg of PE mol ⁻¹ of Zr h ⁻¹)
7	1'·SiO₂(500)	1.2	MAO	270	170
8	1·SiO₂(500)	1.8	none	0	0
9	1·SiO₂(500)	1.8	MAO	260	230
10	1·SiO₂(500)	1.8	B(C ₆ F ₅) ₃	<1	9
11	1·SiO₂(500)/B(C₆F₅)₃^b	1.8	none	80	50

^a Polymerization conditions: 50 °C, 4 bar, 1 h, heptane (300 mL), 200 mg of solid catalyst. MAO assays, [Al]/[Zr] = 500; B(C₆F₅)₃ assays, [B]/[Zr] = 1 with 0.5 mmol/L of TiBA as scavenger. ^b For the synthesis of this surface species, see Experimental Section.

Table 11. Polymerization of Ethylene with Supported **1·Al₂O₃(500)** and **2·Al₂O₃(500)** Catalysts^a

run	catalyst	Zr (%wt)	maximum activity (kg of PE mol ⁻¹ of Zr h ⁻¹)	productivity (kg of PE mol ⁻¹ of Zr h ⁻¹)
12	1·Al₂O₃(500)	0.58	87	70
13	1·Al₂O₃(500)	0.8	76	75
14	1·Al₂O₃(500)	1	109	50
15	1·Al₂O₃(500)	1.4	94	90
16	2·Al₂O₃(500)	1.5	20	13

^a Polymerization conditions: 50 °C, 4 bar, 1 h, heptane (300 mL), 200 mg of solid catalyst.

borane surface species by contacting, just before the catalysis, (≡SiO)ZrCp*Me₂ with 1 equiv of B(C₆F₅)₃ in the reaction solvent.

The catalysts prepared by the first method (run 11) were found to be more active than those prepared in situ (run 10). The catalytic activity and productivity were relatively low compared to those of systems activated with MAO. No improvement was noticed in the catalyst performances when an excess of borane was used (B(C₆F₅)₃/Zr = 10).

Ethylene Polymerization with Alumina-Supported Monocyclopentadienyl Zirconium Catalyst. Contrary to what was observed with (≡Si-O)ZrCp*Me₂, the alumina-supported species exhibited relatively good activity without the addition of any cocatalyst (Table 11). This result was not surprising, taking into consideration the cationic character of some of the alumina-supported zirconium centers. The variation of the zirconium loading in **1·Al₂O₃(500)** complexes (0.58–1.4 wt %) seems to have no significant influence on the activity or production (per mole of Zr) of the catalysts (Table 11, runs 12–15). As previously noticed in the case of solid-phase/gas-phase polymerization (vide supra), the alumina-supported monocyclopentadienyl zirconium complex was found to be more active than the biscyclopentadienyl analogue (run 15 vs 16).

The activity value was still well below that observed for homogeneous systems, so we decided to use a cocatalyst in order to enhance the performance of **1·Al₂O₃(500)** (Table 12). The results obtained in this series of experiments led to several observations. Whatever the cocatalyst used (MAO or B(C₆F₅)₃), the activity of **1·Al₂O₃(500)** increased by a factor about 3. In the case of borane activation, a higher activity was obtained for the isolated **1·Al₂O₃(500)/B(C₆F₅)₃** system (Table 12, runs 18 and 19). In the case of MAO activation, the activity was

quite similar to that observed with silica-supported Cp*ZrMe₃ (Table 12, run 17; Table 10, run 9).

Concerning the characterization of the resulting polymers, we did not succeed in separating the polymer from the inorganic zirconium residue, even under drastic conditions (extraction with hot xylene in a Kumagawa reactor). The lack of solubility of the polymers, observed with both homogeneous and heterogeneous Cp*ZrMe₃, suggests that the molecular weights may be very high. The chain-transfer reactions are apparently highly disfavored for these catalysts.

General Discussion and Conclusion

There is, at the moment, a great interest in industry in developing a heterogeneous process for either ethylene or propylene polymerization with supported metallocenes. There are several reasons but also several requirements for such a need. Mainly, the heterogenization of metallocene catalysts would permit the use of existing gas-phase polymerization technology (no supplementary investments). Another advantage would be to avoid or minimize the use of MAO, the cost of which may be prohibitive. To succeed in such a strategy, the catalyst should have an activity comparable to that of the existing homogeneous systems, while keeping the main characteristics of homogeneous systems regarding polymer microstructure and properties. Such a requirement means that it would be advantageous to keep on the surface the concept of the *single-site character of the active species*.

This work is the result of a conceptual catalyst design based on the strategy of surface organometallic chemistry: starting from the “well-known” structure of the single-site molecular catalysts, one constructs at the surface of an oxide a coordination sphere which responds both to the requirements of molecular coordination sphere and to the grafting process (vide supra).

It is obvious that the objective corresponding to such a strategy was not to achieve on the first attempt the best supported catalyst, but rather to try to establish a structure–activity relationship for a rational understanding of the best methodology to support a Ziegler catalyst. Excellent works have already appeared in this area, showing, for example, that supported, weakly coordinated cationic species can be obtained and give excellent results.¹⁵

We have described in this paper how it is possible to synthesize “relatively well defined” mono- and biscyclopentadienyl complexes of zirconium, using silica, silica–alumina,

Table 12. Polymerization of Ethylene with Supported **1·Al₂O₃(500)** Catalyst^a

run	catalyst	Zr (%wt)	cocatalyst	maximum activity (kg of PE mol ⁻¹ of Zr h ⁻¹)	productivity (kg of PE mol ⁻¹ of Zr h ⁻¹)
15	1·Al₂O₃(500)	1.4		94	90
17	1·Al₂O₃(500)	1.4	MAO	280	260
18	1·Al₂O₃(500)	1.4	B(C ₆ F ₅) ₃	200	190
19	1·Al₂O₃(500)/B(C₆F₅)₃^b	1.4		310	290

^a Polymerization conditions: 50 °C, 4 bar, 1 h, heptane (300 mL), 200 mg of solid catalyst. MAO assays, [Al]/[Zr] = 500; B(C₆F₅)₃ assays, [B]/[Zr] = 1 with 0.5 mmol/L of TiBA as scavenger. ^b See Experimental Section.

and alumina as supports and Cp^*ZrMe_3 and Cp_2ZrMe_2 as molecular precursors. This discussion will consider each complex separately in terms of the structure–activity relationship.

I. Structure. Oxide-Supported Monocyclopentadienyl Zirconium Alkyl Complexes. The first complex that has been fully characterized was obtained by reaction of Cp^*ZrMe_3 with a partially dehydroxylated silica, $\mathbf{1}\cdot\text{SiO}_2$ (**500**). A structure was determined in which the zirconium atom was surrounded by one Cp^* ligand and two methyl groups and linked to the surface via one covalent Si–O–Zr bond.

The grafting reaction leads to the formation of a single surface species which obviously exhibits a neutral character. The surface organometallic complex has two possible propagating centers and one Cp^* ligand. The link with the surface occurs only via one oxygen–zirconium bond and results in a 12-electron species which should give some electrophilic character. Concerning the catalytic results obtained in ethylene polymerization, this surface complex is totally inactive. This behavior is not really surprising, considering the double role of MAO in molecular metallocene chemistry. Obviously, the surface of silica does not exhibit enough Brønsted or Lewis acidity to make a cationic entity.

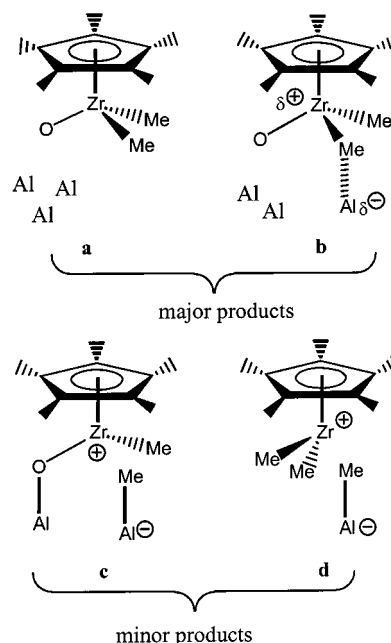
Interestingly, and as expected from homogeneous catalysis, addition of two different cocatalysts (MAO (Al/Zr = 500) or $\text{B}(\text{C}_6\text{F}_5)_3$ (B/Zr = 1)) renders this neutral system active for ethylene polymerization. The level of activity (Table 10) is respectively 230 kg of PE mol^{-1} of Zr h^{-1} for MAO and 50 kg of PE mol^{-1} of Zr h^{-1} for $\text{B}(\text{C}_6\text{F}_5)_3$. We shall see in another publication on this work⁷² that interaction of this neutral complex with $\text{B}(\text{C}_6\text{F}_5)_3$ leads to formation of the surface cationic complex $[\equiv\text{Si}-\text{O}-\text{ZrCp}^*\text{Me}]^+$. This result is further evidence, *but this time on a support*, in favor of the role of Lewis acids as promoters of cationic character of the grafted complex associated with catalytic activity. However, despite this cationic character, the level of activity is still much lower than that of the classical homogeneous metallocene complexes. For example, the molecular complex Cp^*ZrMe_3 associated with MAO gives under comparable experimental conditions (Table 9, run 2) an activity of 3.2×10^3 kg of PE mol^{-1} of Zr h^{-1} . This difference in activity will be discussed later in this paper.

The second surface complex that has been synthesized was obtained by reacting Cp^*ZrMe_3 with a partially dehydroxylated silica–alumina (25% Al), $\mathbf{1}\cdot\text{SiO}_2\text{-Al}_2\text{O}_3$ (**500**). The chemical formula of the resulting surface organometallic complex is identical to the previous one; however, the structure at the molecular level is slightly different (Scheme 1). Solid-state ^{13}C NMR spectroscopy shows that a very small amount of methyl groups of the grafted species interacts with the few Lewis acid sites of the surface, creating thus for a minority of the complex a partial (or total) cationic charge at zirconium (peak at -4 ppm for the corresponding $[\text{Al}-\text{Me}]^-$ and/or $\text{Zr}-(\mu\text{-CH}_3)-[\text{Al}]$ entities).

The activity of this grafted complex remained very low and could not be measured precisely. This low activity can easily be related to the low concentration of the cationic or “cation-like” zirconium species present on silica–alumina.

The third surface complex that we have constructed was obtained by reacting Cp^*ZrMe_3 with a partially dehydroxylated alumina(**500**), $\mathbf{1}\cdot\text{Al}_2\text{O}_3$ (**500**). Here, also, the chemical formula of the surface organometallic fragment was identical to the

Scheme 8



previous ones, $[\text{Al}]_x\text{-OZrCp}^*\text{Me}_2$, with one Cp^* ligand and two methyl groups at zirconium. However, the ^{13}C NMR and EXAFS data gave stronger evidence for the real surface microstructure. ^{13}C NMR showed unambiguously the coexistence of several environments for the zirconium (Scheme 8). Some of the methyl groups interact with acidic Lewis aluminum sites (peak at -11 ppm for the $[\text{Al}-\text{Me}]^-$ moiety, peak at 42 ppm for the $[\text{Zr}-\text{Me}]^+$ moiety) (Scheme 8, **b**, **c**, and **d**). However, not all of the methyl coordinated to Zr can find in the surface environment an aluminum Lewis center at a proper distance so that some neutral complex still coexists on the surface (peak at 35 ppm for the neutral Zr–Me moiety) (Scheme 8, **a**). EXAFS data clearly demonstrate that species **c** and **d** do not seem to be the major structures (Zr–O 2.01 Å, coordination number 1; Zr– C_{sp^3} 2.18 Å, coordination number 1.8; Zr– C_{sp^2} 2.55 Å, coordination number 4.6). Briefly stated, two major structures can be derived from the ^{13}C NMR and EXAFS data: the first one, $[\text{Al}]_3\text{-OZrCp}^*\text{Me}_2$, exhibits a neutral character and the second one, $[\text{Al}]_2\text{-OZrCp}^*\text{Me}(\mu\text{-Me}-[\text{Al}])$, presents a “cation-like” character.

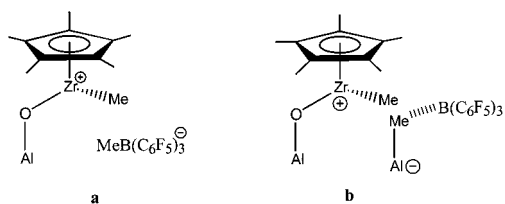
The level of activity of the corresponding complex is 90 kg of PE mol^{-1} of Zr h^{-1} in the absence of any cocatalyst. This result is also in agreement with the molecular concept that a partial (or total) transfer of one methyl to the Lewis center at the surface is a requirement for catalytic activity. Since we have not carried out poisoning experiments, it is difficult to completely rule out species **c** or **d** as the active ones. However, their concentration is very low, as determined by EXAFS.

The level of activity of the supported alumina complex remains low by comparison with that of the homogeneous systems (35 times lower). This can be due to a real surface ligand effect or to the low concentration of truly supported cationic structure.

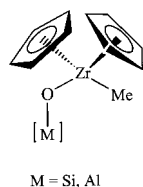
As in the case of silica, addition of MAO (MAO/Zr = 500) or $\text{B}(\text{C}_6\text{F}_5)_3$ (B/Zr = 1) increases the activity by a factor of ca. 3: 260 kg of PE mol^{-1} of Zr h^{-1} for MAO and 290 kg of PE mol^{-1} of Zr h^{-1} for $\text{B}(\text{C}_6\text{F}_5)_3$. Interestingly, the quasi identity of these rates would seem to indicate that both cocatalysts lead to similar coordination spheres in similar concentrations. Since there is 1 equiv of boron per zirconium, the removal and/or

(72) Supported Metallocene Catalysts by Surface Organometallic Chemistry. Synthesis and Characterization of “Cation-like” Heterogeneous Olefin Polymerization Catalysts Based upon Supported Silica and Alumina Cp^*ZrMe_3 and $\text{B}(\text{C}_6\text{F}_5)_3$. Jezequel, M. Ph.D. Thesis, Université Claude Bernard, Lyon I, No. 230-99, 1999.

Scheme 9



Scheme 10



complexation of only one methyl group to the molecular Lewis center is sufficient to get the same activity as 500 equiv of MAO! There are several possibilities which can explain the role of the boron compound, such as the abstraction of one methyl from the neutral complex to create, as on silica, the cationic-like complex $[Al]_x-OZrCp^*Me^+$ (Scheme 9, **a**), or perhaps the complexation of the bridged methyl, leading to, perhaps, its total removal from zirconium (Scheme 9, **b**).

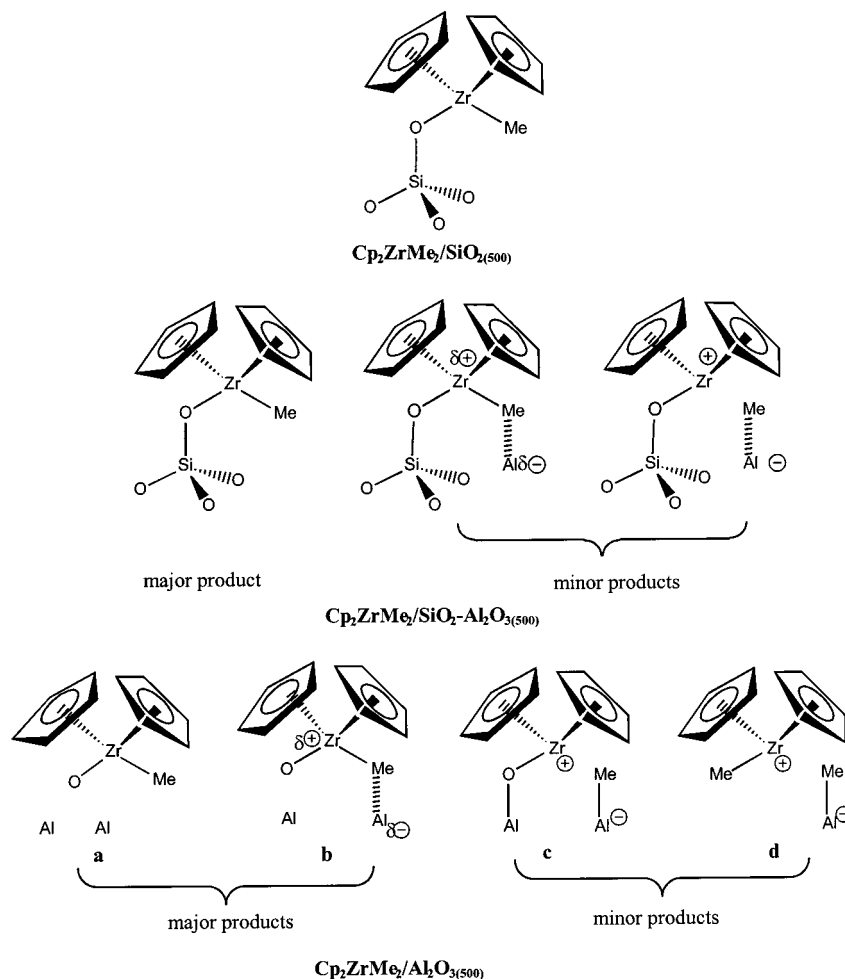
Oxide-Supported Biscyclopentadienyl Zirconium Alkyl Complexes. With biscyclopentadienyl zirconium complexes, the reaction with partially dehydroxylated silica, silica–alumina, and γ -alumina led to the formation of grafted species having

an identical chemical formula: two cyclopentadienyl ligands and one methyl group per zirconium atom and one covalent link via an M–O bond (Scheme 10).

^{13}C NMR and EXAFS of the grafted species have shown various microenvironments on different supports (Scheme 11).

On silica, **2·SiO₂(500)**, we have a neutral complex σ -bonded via one oxygen atom. This 16-electron complex exhibits no catalytic activity in ethylene polymerization. This result has to be compared with the absence of activity of the silica-supported monocyclopentadienyl zirconium complex. On silica–alumina, **2·SiO₂-Al₂O₃(500)**, the 1H NMR shows some interactions of the only methyl group left with some acidic Lewis sites on the silica–alumina surface. The fact that this system exhibits some activity would indicate that a bridging methyl can be the propagating center. On alumina, **2·Al₂O₃(500)**, EXAFS data have shown that the first coordination sphere of the obtained surface species was composed of one oxygen atom ($d_{Zr-O} = 1.98 \text{ \AA}$), one sp^3 carbon atom ($d_{Zr-C} = 2.18 \text{ \AA}$), and ca. 10 sp^2 carbon atoms ($d_{Zr-C} = 2.58 \text{ \AA}$). The methyl group left seems to be either free or partially transferred to an aluminum center (^{13}C chemical shifts at 30 and -11 ppm). Correlation between EXAFS and ^{13}C NMR indicates as major products of the reaction the microstructures **a** and **b** given in Scheme 11. The level of activity of this complex is 13 kg of PE mol^{-1} of Zr h^{-1} . This is a factor of 7 lower than the activity of the monoCp* analogue. We expected that the grafted biscyclopentadienyl complexes should have no activity (impossible for a d^0 Zr(IV) center to accommodate simultaneously one σ -bonded oxygen, two Cp ligands, one methyl group, and a cationic charge). The

Scheme 11



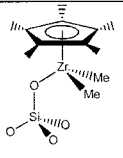
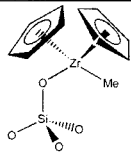
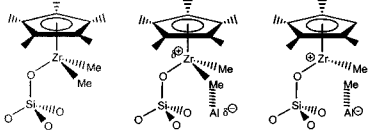
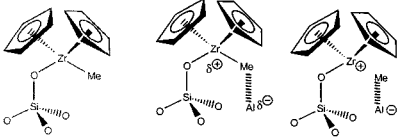
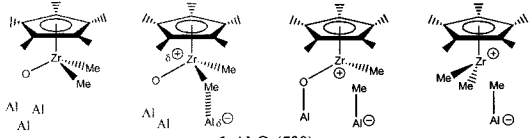
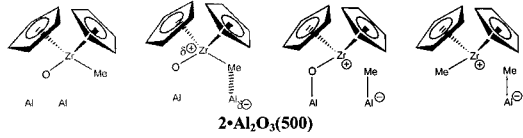
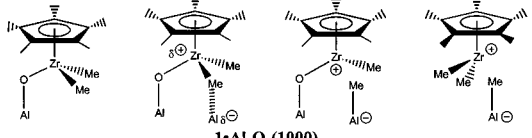
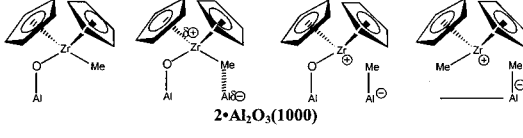
Series MonoCp*	Activity from 0 to +++++		Series BisCp
 1•SiO₂(500)	0	0	 2•SiO₂(500)
 1•SiO₂-Al₂O₃(500)	++	+	 2•SiO₂-Al₂O₃(500)
 1•Al₂O₃(500)	+++++	+++	 2•Al₂O₃(500)
 1•Al₂O₃(1000)	++++	++	 2•Al₂O₃(1000)

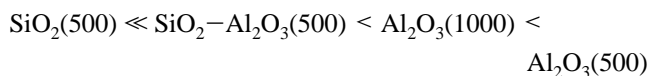
Figure 7. Structure–activity relationship.

fact that there is a much lower activity than with the corresponding monocyclopentadienyl analogue is, to some extent, very logical. The small degree of activity observed suggests that the propagation occurs either on a Zr–Me–Al bond (Scheme 11, **b**) or on a Zr–Me bond of a true cationic species (present in a minute amount, as shown by EXAFS), resulting from the abstraction of a methyl group from the starting molecular complex (Scheme 11, **d**).

II. Activity. Ethylene Polymerization with No Cocatalyst.

When comparing the relative performances of our supported mono- and biscyclopentadienyl zirconium catalysts in the absence of additional cocatalysts (Figure 7), we have noticed that the activity dramatically depends on the choice of the support.

When grafted on a neutral oxide such as silica(500), the zirconium complexes (mono- and biscyclopentadienyl) exhibited no activity at all in ethylene polymerization. When the oxide bore some acidic Lewis centers, the resulting surface species were shown to present some activity. This activity was dependent on the support used and its thermal treatment. Regardless of the type of the starting zirconium complex, mono- or biscyclopentadienyl, the following order of activity has been established:



This order can be directly related to the number of acidic Lewis centers present on the oxides and to the strength of the Lewis acidity of these sites.

The absence of activity in ethylene polymerization observed for the silica-supported zirconium complexes was related to the neutral character of the surface species. The activity, although low in certain cases, observed for the silica–alumina- and alumina-supported species was attributed to the presence of some “cation-like” surface species.

Nevertheless, the activity obtained for the best catalyst, **1•Al₂O₃(500)**, remained very low by comparison to the level of activity reported for the homogeneous systems. By associating ¹³C NMR and EXAFS spectroscopy, we have demonstrated that total transfer of a methyl group from the zirconium to a Lewis acidic aluminum site on the surface is difficult. Thus, fully reactive cationic zirconium complexes were either not present or very rare on the surface, explaining the low activity observed.

It is worth noting that the activities obtained in the series of biscyclopentadienyl zirconium complexes were much lower, whatever the oxide used, than the activities found for the monocyclopentadienyl analogues. This was not surprising, given the inability of this precursor to form a complex having simultaneously a covalent link with the surface, a propagating center, and a full cationic charge at zirconium.

Ethylene Polymerization in the Presence of a Cocatalyst.

The influence of the use of a cocatalyst on the catalytic activity was studied for two surface complexes: **1•SiO₂(500)** and **1•Al₂O₃(500)**. In both cases, the activity was greatly improved by the addition of cocatalysts such as MAO or B(C₆F₅)₃. In the case of the silica-supported complex, a higher activity was found with MAO than with B(C₆F₅)₃. In the particular case of the complex supported on alumina, we observed similar activities for both cocatalysts.

The increase in activity for both supported complexes was interpreted as resulting from a higher concentration of fully cationic zirconium surface complexes (the cocatalyst may either abstract a methyl group from a neutral complex or help in the total displacement of a methyl group already bridged between the grafted zirconium and an aluminum center of the surface).

The activity of the supported zirconium complexes, although improved by the addition of cocatalysts, remained very low by comparison with the homogeneous metallocene systems. This trend has been reported in many works dealing with immobilized metallocenes.^{12b,e,14a,15d} Several explanations can be considered. It may be that an oxide surface is not a favorable ligand for a

polymerization catalyst. The surface would, indeed, occupy a significant portion of the coordination sphere, which may restrict olefin coordination. The siloxy and aluminosy ligands are potentially efficient π -donor ligands, which could greatly reduce the electrophilicity of the zirconium center (the aluminosy would be less donating than the siloxy). However, more sophisticated explanations must be given, considering the very high productivity of group 4 *ansa*-cyclopentadienyl amido catalysts.^{2c} Catalyst mobility may also be a factor: the greater mobility of molecules in solution than on supported complexes probably results in higher activity. It may be also that, in the case of supported metallocenes, the formation of active sites is less efficient.

Considering all these aspects, it seems to us that a direct covalent link between the zirconium complex and an oxygen atom of the surface is not really conducive to olefin polymerization. Given our results, it appears that, to design an efficient catalyst, several features have to be included: the formation of a fully cationic zirconium complex with charge separation, a weaker link with the surface leading to increase zirconium mobility, and a coordination sphere around the zirconium atom, which excludes the presence of oxygen-donating ligands.

Experimental Section

Infrared spectra were recorded on a Nicolet 550-FT by using an infrared cell equipped with CaF₂ windows, allowing in situ studies. Typically 16 scans were accumulated for each spectrum (resolution, 2 cm⁻¹).

All solid-state NMR spectra were recorded on a Bruker DSX-300 spectrometer equipped with a standard 4-mm double-bearing probe head and operating at 75.47, 78.17, and 300.18 MHz for ¹³C, ²⁷Al, and ¹H, respectively. The samples were introduced in the rotor made of zirconia in a glovebox and tightly closed. Boil-off nitrogen was used for both bearing and driving the rotors. For ¹³C NMR, a typical cross-polarization sequence was used: 90° rotation of the ¹H magnetization (impulsion length, 3.8 μ s), and then contact between carbon and proton during $T_c = 5$ ms, and finally recording of the spectrum under high-power decoupling. The delay between each pair of scans was fixed to 2 s, to allow for the complete relaxation of the ¹H nuclei. Chemical shifts are given with respect to TMS by using adamantane as an external reference ($\delta = 37.7$ ppm for the highest chemical shift). The ²⁷Al MAS NMR spectra were recorded by using a single impulsion sequence. The delay between each pair of scans was 1 s, and the number of scans was typically 500. The chemical shifts are given relative to Al(H₂O)₆(NO₃)₃ (1 M) used as an external reference.

Solution NMR spectra were recorded on a AM-300 Bruker spectrometer. All chemical shifts were measured relative to residual ¹H or ¹³C resonances in the deuterated solvents: C₆D₆, δ 7.15 ppm for ¹H, 128 ppm for ¹³C.

X-ray absorption spectra were recorded on Station 9.2 of the Synchrotron Radiation Source at the Daresbury Laboratory (operating at 2 GeV with an average current of ca. 180 mA) using a Si(220) order-sorting monochromator. Samples for EXAFS analysis were prepared and handled under the strict exclusion of air and loaded under nitrogen into airtight aluminum cells equipped with Kapton windows. Spectra were acquired at room temperature in transmission mode. Background-subtracted EXAFS data were obtained using the program PAXAS.⁷³ Spherical wave curve-fitting analysis was executed in EXCURV98,^{74,75} using ab initio phase shifts and backscattering amplitudes calculated using Von-Barth ground-state potentials and Heding–Lundqvist exchange potentials. The k^3 -weighted parameters are presented in Table

(73) Binsted, N. *PAXAS Program for the Analysis of X-ray Absorption Spectra*; University of Southampton, UK, 1988.

(74) (a) Gurmman, S. J.; Binsted, N.; Ross, I. J. *Phys. Chem.* **1984**, *17*, 143. (b) Gurmman, S. J.; Binsted, N.; Ross, I. J. *Phys. Chem.* **1986**, *19*, 1845.

(75) Binsted, N. *EXCURV98*; CCLRC Daresbury Laboratory computer program, 1998.

2. The accuracy of bonded and nonbonded interatomic distances was considered to be 1.4% and 1.6%, respectively.⁵² Precisions on first-shell coordination numbers are estimated to be ca. 10% and between 10 and 20% for nonbonded shells. The *R* factor is defined as

$$\left(\int [\chi^T - \chi^E] k^3 dk / [\chi^E] k^3 dk \right) \times 100\%$$

where χ^T and χ^E are the theoretical and experimental EXAFS and k is the photoelectron wave vector.

Gas-phase analysis was performed on a Hewlett-Packard 5890 series II gas chromatograph equipped with a flame ionization detector and an Al₂O₃/KCl on fused silica column (50 m \times 0.32 mm). Elemental analyses were performed by the Central Analysis Service of the CNRS at Solaize or at Pascher laboratory (Remagen, Germany) in the case of extremely sensitive products. In this case, samples were transferred to microanalysis sealed tube in the pure atmosphere of a glovebox. Mass spectra (CH₃D/CH₄ ratio determination) were recorded on a 70E Micromass spectrometer with double focalization ($E_i = 70$ eV, 10⁻⁸ mmHg).

Silica (Aerosil from Degussa, 200 m²/g), silica–alumina (Ketjen, 374 m²/g, 25% Al), alumina (Degussa, 100 m²/g), and niobia (Nb₂O₅·*n*H₂O from C.B.M.M., 93 m²/g) were compacted to a disk (30 mg) for infrared studies or were hydrated, dried, and crushed to prepare large quantities (1–1.5 g) for NMR studies and elemental analyses. Before reaction with the molecular zirconium complex, all the oxides were calcinated at 500 °C under a stream of O₂ for 15 h; after cooling at room temperature and evacuation, they were dehydroxylated under vacuum (10⁻⁵ mmHg) for 15 h at the desired temperature (SiO₂(500), SiO₂–Al₂O₃(500), Al₂O₃(500)), except in the case of niobia, which was previously exposed to water (15 Torr, 3 h) and then evacuated at 300 °C overnight.

The solvents were dried and distilled under nitrogen by standard methods prior to use (Et₂O and THF on Na/benzophenone; pentane and heptane on Na/K amalgam).

Cp*ZrCl₃, Cp₂ZrCl₂, Mg, and Li were purchased from Aldrich Chemical and used without further purification. Cp*Zr(CH₃)₃ and Cp₂Zr(CH₃)₂ were prepared according to procedures previously described in the literature.^{31a,59} ¹³CH₃I (¹³C, 99%) and CD₃I (D₃, 99.5%) were obtained from Cambridge Isotope Laboratories.

Ethylene (Air Liquide, >99.95%) was passed through a purification trap containing molecular sieves just before addition to the IR cell. Methylaluminoxane (MAO in toluene, 1.9 M) was purchased from Schering. Triisobutylaluminum (TiBA, Schering) was taken as a 1 M solution in heptane. B(C₆F₅)₃ was purchased from Strem Chemical and used without further purification.

All manipulations were conducted under a strict inert atmosphere or vacuum conditions using, in some cases, Schlenk techniques.

Preparation of Labeled Molecular Precursors. Synthesis of Cp*Zr(¹³CH₃)₃, 1-¹³C. The synthesis of 1-¹³C was achieved in two steps according to procedures described in the literature for similar compounds.^{31a,33}

(a) Preparation of ¹³CH₃MgI. On a suspension of magnesium turnings (1 g, 0.04 mol) in 5 mL of diethyl ether, freshly distilled, was added dropwise under vigorous stirring 1.9 mL (0.03 mol) of ¹³CH₃I in 40 mL of Et₂O. The mixture was then refluxed for 2 h. After cooling, the suspension was filtered to give 30 mL of ¹³CH₃MgI (1 M) in diethyl ether solution (yield >99%).

(b) Preparation of Cp*Zr(¹³CH₃)₃. A diethyl ether solution of ¹³CH₃MgI (5.8 mL, 0.017 mol) was slowly added to a suspension of Cp*ZrCl₃ (1.76 g, 5.3 mmol) in 50 mL of diethyl ether maintained at –78 °C. The mixture was allowed to warm to room temperature and then was stirred 2 h. Diethyl ether was removed under vacuum, and 40 mL of dry pentane was added on the solid to extract the product (this operation was repeated twice). The resulting pentane solution was then filtered and the solvent evacuated under vacuum to give a white solid, identified by ¹H and ¹³C NMR as Cp*Zr(¹³CH₃)₃.

For 1-¹³C: ¹H NMR, C₆D₆, δ 1.77 ppm (s, 15 H, CH₃ of Cp* ligand), 0.23 ppm (d, 9 H, Zr–CH₃, ¹J_{CH} = 114 Hz); ¹³C{¹H} NMR, C₆D₆, δ 11 ppm (s, CH₃ of Cp* ligand), 46 ppm (s, Zr–CH₃ group), 119 ppm (s, C of the Cp* ring).

Synthesis of $\text{Cp}_2\text{Zr}^{13}\text{CH}_3)_2$, $2\text{-}^{13}\text{C}$. The synthesis of $2\text{-}^{13}\text{C}$ was achieved in two steps according to procedures described in the literature.⁵⁹

(a) Preparation of $^{13}\text{CH}_3\text{Li}$. On a suspension of lithium turnings (0.41 g, 0.06 mol) in 30 mL of diethyl ether, freshly distilled, was added dropwise under vigorous stirring 1.9 mL (0.03 mol) of $^{13}\text{CH}_3\text{I}$ in 10 mL of Et_2O . The mixture was then refluxed for 3 h. After cooling, the suspension was filtered to give 39 mL of $^{13}\text{CH}_3\text{Li}\cdot\text{LiI}$ (0.77 M) in diethyl ether solution (yield >99%).

(b) Preparation of $\text{Cp}_2\text{Zr}^{13}\text{CH}_3)_2$. A diethyl ether solution of $^{13}\text{CH}_3\text{Li}\cdot\text{LiCl}$ (15 mL, 11.5 mmol) was slowly added to a suspension of Cp_2ZrCl_2 (1.68 g, 5.75 mmol) in 60 mL of pentane. The mixture was stirred at room temperature for 7 h. Solvents were removed under vacuum, and 60 mL of dry pentane was added on the solid to extract the product (this operation was repeated twice). The resulting pentane solution was then filtered the solvent evacuated under vacuum to give 1.43 g of white solid (yield 98%), identified by ^1H and ^{13}C NMR as $\text{Cp}_2\text{Zr}^{13}\text{CH}_3)_2$.

For $2\text{-}^{13}\text{C}$: ^1H NMR, C_6D_6 , δ -0.19 ppm (d, 6 H, $\text{Zr}-\text{CH}_3$, $^1J_{\text{CH}} = 117$ Hz), 5.7 ppm (s, 10 H, H of Cp ligand); $^{13}\text{C}\{^1\text{H}\}$ NMR, C_6D_6 , δ 30 ppm (s, $\text{Zr}-\text{CH}_3$ group), 110 ppm (s, C of the Cp ring).

Synthesis of Oxide-Supported $\text{Cp}^*\text{Zr}(\text{CH}_3)_3$ and $\text{Cp}_2\text{Zr}(\text{CH}_3)_2$ Complexes: General Procedure. Sublimation Method. **1** and **2** were sublimed (respectively at room temperature and at 60 °C) under vacuum (10^{-5} Torr) onto the oxide previously treated at the desired temperature. The unreacted starting precursors were removed under vacuum by sublimation for 15 h. The grafting reaction was followed by infrared spectroscopy and analysis of the gas phase by GC.

Impregnation Method. A solution of **1** and **2** in dry pentane was added through the filter of a double Schlenk tube to a pentane suspension of the oxide previously dehydroxylated at the desired temperature. After being stirred for 1 h at room temperature, the pentane solution containing the unreacted starting material was filtered to the other side of the Schlenk tube, where the reaction had taken place. The pentane was recondensed on the oxide to further wash the solid and then filtered. This procedure was repeated two more times. Finally, the solid was dried for several hours under vacuum (10^{-2} Torr). The resulting surface species were then characterized by solid-state NMR spectroscopy, and in some case by EXAFS spectroscopy, elemental analyses, and chemical reactivity.

Preparation of $1\cdot\text{SiO}_2(500)/\text{B}(\text{C}_6\text{F}_5)_3$ and $1\cdot\text{Al}_2\text{O}_3(500)/\text{B}(\text{C}_6\text{F}_5)_3$. In a two-sided, fritted reaction vessel, a pentane solution containing a measured quantity of $\text{B}(\text{C}_6\text{F}_5)_3$ was filtered onto an equimolar quantity of $1\cdot\text{SiO}_2(500)$ and $1\cdot\text{Al}_2\text{O}_3(500)$. The resulting slurry was then stirred at room temperature for 1 h. The suspension was then filtered and the solid washed twice with condensed pentane from the filtrate. After being dried under vacuum (10^{-2} Torr, 1 h; 10^{-5} Torr, 2 h), the catalyst was stored at -20 °C in a glovebox.

Polymerization Procedure. Ethylene homopolymerization reactions were performed in a 500-mL pressurized and thermoregulated glass reactor.

(a) Homogeneous Catalysis. A quantity of the homogeneous metallocene dissolved in toluene or heptane (depending on the solubility) was added to a solution of heptane (500 mL) containing $\text{B}(\text{C}_6\text{F}_5)_3$ or MAO. The amount of MAO used in the polymerization experiments corresponded to an Al/Zr ratio of 500. $\text{B}(\text{C}_6\text{F}_5)_3$ was always used stoichiometrically related to zirconium concentration. For the runs without MAO, triisobutylaluminum was taken as scavenger at a concentration of 0.5 mmol/L. These reagents were introduced at room temperature via a cannula under a stream of dry argon. After the removal of argon under vacuum, the reactor was charged with ethylene and heated at 50 °C (this temperature was maintained constant throughout). The ethylene pressure in the reactor (4 bar) was kept constant during the reaction by supplying the monomer from a large volume reservoir through a control valve. The reaction time for all polymerization experiments was 1 h. Ethylene was then degassed, and the polymerization product was stirred with acidified methanol. Finally, the polymer was filtered and washed with ethanol and heptane and dried for 5 h at 100 °C under vacuum.

The activity was followed from the kinetic measurements of the pressure drop in the reservoir. For each run, the activity, expressed in kilograms of PE per mole of Zr per hour, was represented as a function of time. Catalyst productivity (expressed in kilograms of PE per mole of Zr per hour) was calculated from the weight of the polymer obtained.

(b) Heterogeneous Catalysis. The solid catalysts were weighed precisely into the reactor in an argon atmosphere glovebox, and the polymerization procedure was then similar to that described above for the homogeneous systems.

Acknowledgment. The authors thank ELF-ATOCHEM for financial support and constant interest. We also thank EPSRC for support (to S.G.F.), the CLRC Daresbury Laboratory for access to facilities for EXAFS experiments, and Dr. Roger Spitz for his help in the polymerization experiments and very fruitful discussions.

Supporting Information Available: EXAFS spectra for **1**· $\text{Al}_2\text{O}_3(500)$ and **2**· $\text{Al}_2\text{O}_3(500)$; the infrared spectra of **1**· $\text{SiO}_2(500)$, **1**· $\text{SiO}_2\text{-Al}_2\text{O}_3(500)$, **1**· $\text{Al}_2\text{O}_3(500)$, and **1**· $\text{Nb}_2\text{O}_5(300)$; ^{13}C NMR spectra of $2\text{-}^{13}\text{C}$ in the liquid and solid states; infrared spectra of **2** on various oxides; activity vs time plot for the polymerization of ethylene by two homogeneous catalyst systems, $\text{Cp}_2\text{ZrMe}_2/\text{MAO}$ and $\text{Cp}_2\text{ZrMe}_2/\text{B}(\text{C}_6\text{F}_5)_3$; activity vs time plot for the polymerization of ethylene by **1**· $\text{Al}_2\text{O}_3(500)$, **1**· $\text{Al}_2\text{O}_3(1000)$, and **2**· $\text{Al}_2\text{O}_3(500)$; and infrared spectra of the polymerization of ethylene over various oxide-supported bis-cyclopentadienyl zirconium species (PDF). This material is available free of charge via the Internet at <http://pubs.acs.org>.

JA000682Q